

2 up  
NASA CR-130139

036350-3-T

# High Resolution Spectroscopic Measurements of Carbon Dioxide and Carbon Monoxide

Technical Report

LUCIAN W. CHANEY

(NASA-CR-130139) HIGH RESOLUTION  
SPECTROSCOPIC MEASUREMENTS OF CARBON  
DIOXIDE AND CARBON MONOXIDE Technical  
Report (Michigan Univ.) 83 p HC \$7.25  
69

N74-27591

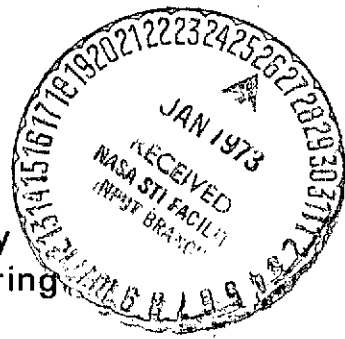
Unclas  
42265

CSSL 07D G3/06

July 1972

National Aeronautics and Space Administration  
Contract No. NSR 23-005-376  
Washington, D.C.

High Altitude Engineering Laboratory  
Departments of Aerospace Engineering,  
Meteorology and Oceanography



THE UNIVERSITY OF MICHIGAN  
COLLEGE OF ENGINEERING  
High Altitude Engineering Laboratory  
Departments of  
Aerospace Engineering  
Meteorology and Oceanography

Technical Report

HIGH RESOLUTION SPECTROSCOPIC MEASUREMENTS  
OF  
CARBON DIOXIDE AND CARBON MONOXIDE

Lucian W. Chaney

ORA Project 036350

under contract with:

NATIONAL AERONAUTICS AND SPACE ADMINISTRATION  
CONTRACT NO. NSR 23-005-376  
WASHINGTON, D C.

administered through

OFFICE OF RESEARCH ADMINISTRATION ANN ARBOR

July 1972

## ACKNOWLEDGMENT

The work described in this report was made possible through the cooperation of the Infrared Laboratory of the Institute of Science and Technology, University of Michigan. The author is particularly grateful to Charles B. Arnold of that laboratory for his many helpful suggestions regarding the instrumentation.

Thanks also go to S. R. Drayson of the High Altitude Engineering Laboratory who contributed the many spectral computer plots.

The work described has been supported by the National Aeronautics and Space Administration Contract No. NSR 23-005-376.

## Table of Contents

	Page
List of Figures	v
Abstract	viii
1.0 Introduction	1
1.1 Purpose	1
2.0 Instrument Description	2
2.1 Instrumentation Component List	3
2.2.0 Tracing Optical Path	5
2.2.1 Source	5
2.2.2 Chopper	6
2.2.3 Sample Cell	7
2.2.4 Entrance Optics	7
2.2.5 Slits	8
2.2.6 Basic Instrument	8
2.2.7 Gratings	9
2.2.8 Exit Optics	10
2.2.9 Detector	11
3.0 Data Recording System	12
3.1 Pre-Amplifier	13
3.2 Phase-Lock Amplifier	13
3.3 Analog Chart Recorder, Leeds and Northrup Speed-O-Max Type 6	13
3.4 Integrating Voltmeter	14
3.5 Digitizing Signals	15
3.6 Computer Outputs	17

## Table of Contents (cont'd)

	Page
4.0 Gas Handling System	17
4.1 Purge Gas	19
5.0 Temperature Control	19
5.1 Room Heaters	19
6.0 Optical Alignment and Set-up	21
6.1 Main Mirror Adjustment	21
6.2 Grating Adjustment	21
6.3 Baffles	22
6.4 Slit Alignment	23
6.5 Input and Exit Optics Adjustment	23
6.6 Image Adjustment	23
6.7 Slit Width Adjustment	24
7.0 Operating Procedures	25
7.1 Data Collection	26
8.0 Data and Measurements	27
8.1 Line Position Measurements ( $15\mu\text{m CO}_2$ )	28
8.2 Isotope Measurements ( $15\mu\text{m CO}_2$ )	28
8.3 Carbon Dioxide $4.3\mu\text{m}$ Band	29
8.4 Carbon Monoxide $4.6\mu\text{m}$ Band	29
8.5 Carbon Monoxide $2.3\mu\text{m}$ Band	29
References	31
Data Summary	

## List of Figures

### Figure

1. Graphite Rod Source
2. Cross-sectional Diagram of Graphite Source
3. Optical Path Diagram of Complete Instrument
4. Sketch of Entrance and Exit Optics
5. Output Optics
6. Grating Sketch, Showing Back Corners Removed
7. Grating Drive Mechanism
8. Detector Bias Circuits
9. Electrical Block Diagram of Complete Instrument
10. Gas Handling System Schematic
11. Gas Manifold
12. Optical Adjustment Laser Pattern
13. Alternate resolution test. Comparison of theoretically computed spectrum (solid line) and measured spectrum (dotted lines). The theoretical resolution is  $0.08 \text{ cm}^{-1}$ . Spectrum is the P and Q branches of band  $[(100:0)\text{I}-010:1]$  centered at  $720.81 \text{ cm}^{-1}$ .
14. Shows portions of the P, Q, and R branches of band  $(010:1-000:0)$  centered at  $667.38 \text{ cm}^{-1}$ .
15. Spectrum of Q branch of band  $[(110:1)\text{II}-(100:0)\text{II}]$  centered at  $647.06 \text{ cm}^{-1}$  and the  $^{13}\text{C}^{16}\text{O}_2$  isotopic Q branch of band  $(010:1-000:0)$ .
16. The spectrum includes the Q branches of band  $[(100:0)\text{I}-010:1]$  centered at  $720.81 \text{ cm}^{-1}$ , the same band for the isotope  $^{13}\text{C}^{16}\text{O}_2$  centered at  $721.59 \text{ cm}^{-1}$ , and the identifiable R branch lines of the weak band  $[(200:0)\text{I}-(110:1)\text{I}]$  centered at  $720.29 \text{ cm}^{-1}$ . The ability to identify the R branch lines demonstrates the excellent signal to noise capability.
17. Spectrum of the Q branch of band  $[(110:1)\text{I}-020:2]$  centered at  $741.72 \text{ cm}^{-1}$  and the Q branch of band  $[(200:0)\text{II}-(110:1)\text{II}]$  centered at  $738.67 \text{ cm}^{-1}$ .

List of Figures (cont'd)

Figure

18. Spectrum of Q branch of band [(120:2)II-030:3] centered at  $581.7 \text{ cm}^{-1}$  in a region of poor signal to noise ratio.
19. Long path spectrum ( $634 \text{ cm}^{-1}$ - $641 \text{ cm}^{-1}$ ) which demonstrates the large number of lines which can be separated. Virtually every feature on the spectrum can be identified as a spectral line.
20. Spectrum of the Q branch of band [(100:0)II-010:1] centered at  $618.03 \text{ cm}^{-1}$ .
21. Example of how strong lines stand out in a noisy spectrum. The spectrum is dominated by the P branches of bands [(100:0)II-010:1] and [(110:1)II-020:2]
22. Spectrum near  $770 \text{ cm}^{-1}$ . The strongest absorption lines are the R branch of band [(100:0)I-010:1] centered at  $720.81 \text{ cm}^{-1}$  and band [(110:1)I-020:2] centered at  $741.72 \text{ cm}^{-1}$  and the P branch of band [(110:1)I-(100:0)II] centered at  $791.45 \text{ cm}^{-1}$ . The anomalous feature at  $771.3 \text{ cm}^{-1}$  is due to the unresolved lines of the Q branch of  $^{13}\text{C}^{16}\text{O}_2$  band [(110:1)I-100:0)II].
23. The spectrum demonstrates the background variation problem due to the interference filter. The principal features are the Q branch of band [(120:2)I-(110:1)II] centered at  $823.23 \text{ cm}^{-1}$  and the R branch of [(110:1)I-(100:0)II] centered at  $791.45 \text{ cm}^{-1}$
24. Spectrum enriched in  $^{13}\text{C}^{16}\text{O}_2$  shows Q branch of (010:1-000:0) centered at  $648.48 \text{ cm}^{-1}$ .
25. Spectrum enriched in  $^{13}\text{C}^{16}\text{O}_2$  showing Q branch of band [(100:0)II-010:1].
26. Spectrum enriched in  $^{13}\text{C}^{16}\text{O}_2$  showing Q branch of band [(100:0)I-010:1].
27. Spectrum enriched in  $^{13}\text{C}^{16}\text{O}_2$  in 8.74 cm cell, pressure 75 torr, temperature  $24^\circ\text{C}$  and normal  $\text{CO}_2$  placed in 20 meter cell, pressure 2.4 torr. Resolution reduced to  $0.08 \text{ cm}^{-1}$  to improve signal noise ratio.
28. Spectrum enriched in  $^{13}\text{C}^{16}\text{O}_2$  in 8.74 cm cell, pressure 150 torr, temperature  $24.5^\circ\text{C}$ . Normal  $\text{CO}_2$  in 20 meter cell, pressure 2.4 torr. The Q branches are band [(100:0)I-(010:1)]
29. Spectrum enriched in  $^{18}\text{O}$ . The prominent features are due to the  $\nu_2$  fundamental Q branches of the isotopic molecules  $^{12}\text{C}^{18}\text{O}_2$ ,  $^{12}\text{C}^{16}\text{O}^{18}\text{O}$ , and  $^{12}\text{C}^{16}\text{O}_2$ .

## List of Figures (cont'd)

### Figures

30. Spectrum enriched in  $^{18}\text{O}$ . The strongest lines are due to the  $\nu_2$  fundamental and demonstrates the many lines which can be separated.
31. Spectrum enriched in  $^{17}\text{O}$  and  $^{18}\text{O}$ . The spectrum shows the Q branches of the  $\nu_2$  fundamental of the following isotopic molecules:  $^{12}\text{C}^{18}\text{O}_2$ ,  $^{12}\text{C}^{17}\text{O}^{18}\text{O}$ ,  $^{12}\text{C}^{16}\text{O}^{18}\text{O}$ ,  $^{12}\text{C}^{17}\text{O}_2$ ,  $^{12}\text{C}^{16}\text{O}^{17}\text{O}$  and  $^{12}\text{C}^{16}\text{O}_2$ .
32. Spectrum near the band center of the  $\nu_3$  fundamental of  $\text{CO}_2$ . An example of the spectrum obtained during the self-broadening study.
33. Background or 100% transmission spectra used to normalize Fig. 32. Demonstrates the noise level obtained.
34. The R branch of the  $\nu_3$  fundamental used for the self-broadening study. The isotopic and "hot" bands seen in Fig. 32 are weak in this region.
35. An example of nitrogen broadening in the same spectral region as Fig. 34.
36. Spectra of the  $\text{R}_{20}$  Line of the  $4.6\mu\text{m}$  Band of CO, Self Broadening Study.
37. Spectra of the  $\text{R}_{10}$  Line of  $4.6\mu\text{m}$  Band of CO Nitrogen Broadening Study.
38. Spectra of  $\text{R}_1$  Line of  $4.6\mu\text{m}$  Band of CO Nitrogen Broadening.
39. Example of a Partial Spectrum of the  $2.3\mu\text{m}$  Band of CO across the Center of the Band.



## ABSTRACT

This report describes a modified 1.83 meter Jarrell-Ash spectrometer. The instrument was double passed and achieved a resolution of  $0.05 \text{ cm}^{-1}$  at  $15\mu\text{m}$ . The instrument makes use of an H. P. 2401C Integrating Voltmeter to optimize the available integration time.

Data was obtained in the  $15\mu\text{m}$  and  $4.3\mu\text{m}$  band of  $\text{CO}_2$  and the  $4.6\mu\text{m}$  and  $2.3\mu\text{m}$  bands of  $\text{CO}$ . The data is summarized and examples of typical spectrum are given. All the data is stored on IBM cards. Copies of any spectrum will be available upon request until March 1, 1973.

## 1.0 Introduction

The high resolution spectroscopic measurements described are part of a long term effort by the High Altitude Engineering Laboratory to develop meteorologically significant satellite radiation measurements. Past efforts were directed towards instrument developments, particularly the IRIS interferometer, and high altitude balloon testing of other radiation measuring instruments. The most promising experiment has been the "Kaplan" <sup>1</sup> radiation inversion experiment to obtain temperature profiles. Theoretical work by Drayson <sup>2</sup> indicated that improved transmissivities in the  $15\mu\text{m}$   $\text{CO}_2$  band would be useful.

The desirability of obtaining more accurate transmissivities was apparent several years ago. The High Altitude Engineering Laboratory initially attempted to obtain funding for the purchase of a high resolution spectrometer, but was unsuccessful. In the spring of 1969 an instrument located in the Infrared laboratory of the U. of M. Institute of Science and Technology became available. Funding was obtained from NASA Goddard to modify the instrument for our purpose and make measurements in the  $15\mu\text{m}$  band of  $\text{CO}_2$ .

Once the instrument was set up for the  $15\mu\text{m}$  measurements, it was determined that by changing the detector and order sorting filter, measurements could be obtained in the  $4.3\mu\text{m}$  band of  $\text{CO}_2$ . Finally, because of the continued availability of the instrument, funding was obtained from NASA-Langley to make measurements in the  $4.6\mu\text{m}$  and  $2.3\mu\text{m}$  bands of  $\text{CO}$ .

## 1.1 Purpose

The fundamental purpose of the report is to describe the high resolution spectrometer, the measurement procedure, and provide a permanent

record of the data. The data obtained are currently being analyzed and the results will be reported separately as scientific papers, thesis, or both.

The reports and analysis scheduled thus far are as follows:

- 1) Complete frequency analysis of the  $18\mu\text{m} - 12\mu\text{m}$   $\text{CO}_2$  band by Dr. Roland Drayson.
- 2) Analysis of isotopic  $15\mu\text{m}$  bands of  $\text{CO}_2$  — doctoral dissertation by James B. Russell.
- 3) Strength and line width determinations of the  $4.3\mu\text{m}$  band of  $\text{CO}_2$  by Dr. Roland Drayson.
- 4) Strength and line width determination of the  $4.6\mu\text{m}$  band of CO — doctoral dissertation by Raja Tallamaraju.
- 5) Strength and line width determination of  $2.3\mu\text{m}$  band of CO — investigator to be selected.

The report will serve as a reference for those doing the theoretical analysis and hopefully answer questions regarding the instrument and measurement procedure.

## 2.0 Instrument Description

The basic instrument is a 1.83m Fastie-Ebert vacuum scanning spectrometer built by the Jarrell-Ash Co. The instrument effective aperture ratio is  $F/11.6$ . The theoretical resolution at the  $16\mu\text{m}$  blaze angle is  $0.027\text{cm}^{-1}$  and the measured resolution was  $0.05\text{cm}^{-1}$ . The data scan rate was 220 seconds per wave number, except for the  $2.3\mu\text{m}$  data which was 110 seconds per wave number.

The procedure to be followed in describing the instrumentation will be to first list the components of the system and the manufacturers.

The component list is followed by a system description starting from the source and tracing the signal through to the detector.

## 2.1 Instrumentation Component List

1. Basic Instrument: Jarrell-Ash Mod. 78-400. Main vacuum tank 80" long x 18" OD x 3/8 wall evacuable to a standard leak rate of less than  $10^{-10}$  standard cc/second.

Main mirror concave spherical 16" diameter aluminized surface—  
1. 83m focal length. Jarrell-Ash grating holder 11-006. Jarrell-Ash grating drive 78-404 high precision measuring engine with 12 speed reversible linear drive. Drive screw has a 1mm pitch, constant to  $3\mu\text{m}$  over the 240mm length, and a periodic error of less than  $1\mu\text{m}$ . Engine has 'V' and flat ways carrying an optically flat glass drive plate.

2. Bausch and Lomb grating Cat. No. 35-53-920-27

Blaze =  $16\mu\text{m}$                       Blaze angle =  $28^{\circ}41'$   
Grooves/mm = 60                      Ruled area = 128mm x 206mm  
Bausch and Lomb grating Cat. No. 35-53-860-27  
Blaze =  $4.0\mu\text{m}$                       Blaze angle =  $17^{\circ}27'$   
Grooves/mm = 150                      Ruled area = 128mm x 206 mm.

3. Vacuum pumps

Welch mod. 1397B-500 lpm,  $1 \times 10^{-4}$  torr for main tank  
Welch mod. 1405H-35 lpm,  $5 \times 10^{-5}$  torr for gas cells.

4. Detectors

- 1) Texas Instruments type GCC 8142 (2mm x 0.25mm sensitive area) copper doped germanium mounted in a Linde IR-15 dewar. Used for  $15\mu\text{m}$  measurements.

- 2) Texas Instruments type 15V 8142 (2mm x 0.25mm area) Indium antimonide mounted in an Linde IR-15 dewar. Used for 4.3 $\mu$ m and 4.6 $\mu$ m measurements.
- 3) Eastman Lead Sulfide mounted in an Linde IR-10 dewar. Used for 2.3 $\mu$ m measurements.
5. Interference Filters  
Optical Coating Laboratory
  - 1) 11 $\mu$ m low pass for 15 $\mu$ m data
  - 2) 3.6 $\mu$ m - 5.2 $\mu$ m band pass for 4.3 $\mu$ m and 4.6 $\mu$ m data
  - 3) 2.07 $\mu$ m - 2.708 $\mu$ m band pass for 2.3 $\mu$ m data
6. Pre-Amplifier - Ithaco Mod. 112
7. Phase-Lock Amplifier - Princeton Applied Research Co. Mod. 120
8. Analog Amplifier and Recorder - Leeds & Northrup Speed-O-Max Type G
9. Card Punch Coupler - Hewlett-Packard Mod. 2526
10. Integrating Digital Voltmeter - Hewlett-Packard Mod. DY 2401C
11. Audio Oscillator - Wavetex Mod. 111
12. Card Punch - IBM Printing Summary Punch No. 526
13. Resistance Bridge - Leeds & Northrup Mod. 5305
14. MKS - Baratron pressure gage Mod. 77
15. Regulated Power Supply - Sorenson Mod. R5010 120 Volts 63 amps.
16. Variac, 2-gang - 50 amp. General Radio
17. Power current step up transformer. 6 to 1 Max 600 amps Osborne Transfer Co. Mod. 69353 - 7500 VA
18. University of Michigan Designed and Built Components
 

Source - Graphite Rod Resistance	Figure 1
Chopper - 90 cycle	Figure 3

Input optics	Figure 3
Exit optics	Figure 3
Slits, input and exit	Figure 4
Double Pass Adaption	Figure 5
Signal Digitizer	Figure 7
Gas Handling System	Figure 10

## 2. 2. 0 Tracing Optical Path

### 2. 2. 1 Source

Two sources were used for the measurements.

- 1) the graphite rod source was used for the  $15\mu\text{m}$ ,  $4.6\mu\text{m}$  and  $4.3\mu\text{m}$  measurements.
- 2) a 600 watt tungsten-iodide lamp made by General Electric was used for the  $2.3\mu\text{m}$  measurements.

The graphite rod source (Fig. 1) was designed and built by the U. of M. Infrared laboratory. The rod, which is mounted inside a water cooled housing, is heated electrically. The nominal heating current was 250 amps. If required, the current can be increased to 400 amps.

In order to minimize the noise from the source, the primary power is regulated by a 120 volt 63 amp Sorenson supply. The regulated power is fed to a General Radio Variac - two 50 amp regulators ganged together. (Fig. 2) The Variac voltage setting varied from 63 volts when the source was new to 95 volts just prior to burn out.

The Variac drives the source power transformer. The secondary winding is made of  $1/2''$  diameter copper tube. The tubing is connected to the water cooled jacket surrounding the graphite rod. The "O" rings which prevent the water from reaching the rod also insulate the housing from the rod. Hence,

the cooling water flows through the secondary winding without shorting the graphite source. The operating source temperature was  $1900^{\circ}\text{K}$ . Rapid oxidation of the source is prevented by a purge of 99.998% pure argon. The purge rate was 2 lpm. The argon flowed into the back of the source housing and out through a small hole directly behind the KBr lens.

The limited source life is due to the water vapor escaping under the "O" rings into the source compartment. The water vapor and hot carbon form both carbon dioxide and carbon monoxide. During some of the CO measurements it was necessary to raise the argon flow rate to completely eliminate the CO from the light path.

The quartz iodide lamp source used for the  $2.3\mu\text{m}$  measurements was operated from the same regulator and a smaller variac. The source was focused by means of an off-center ellipse on the input window of the spectrometer. The window image was twice the source height.

The energy from the graphite source was focused by a 6.0 cm focal length KBr lens on the input window. The source to lens distance was 9.0 cm and the lens to window distance was 18.0 cm.

### 2.2.2 Chopper

The 90 cycle chopper was mounted directly in front of the lens. The 8.74 cm sample cell was located between the chopper and the spectrometer entrance window. The distance between the chopper and the cell and between the cell and entrance window was about 2 cm each. This area was purged with the boil off from a liquid nitrogen storage tank. Plastic wrap and masking tape were used to seal the open areas, making the purge more effective.

The chopper blade was 8 inches in diameter and notched every  $60^{\circ}$ , making the chop rate three times the rotation rate. The chopper was

driven by a Bodine KYC-24-P1 synchronous motor. Since the motor was designed for a smaller blade, the torque was insufficient to reach synchronous speed. The problem was solved by using a Variac to raise the starting voltage to 140 volts.

The chopper also generated the reference square wave which was fed to the phase lock amplifier. The bulb and the photocell used to generate the signal were mounted in the housing diametrically opposite the measured beam. The pulse shaping circuit was mounted in a small box attached to the housing.

### 2.2.3 Sample Cell

The sample cell was located between the chopper and the input window. The optical path length was 8.74 cm and the inside diameter 4.0 cm. The windows were 6 mm thick and made of KBr. The cell material was stainless steel. The cell was connected by 1/4 inch stainless steel tubing to the gas manifold. The manifold and gas handling procedure will be discussed later.

The 8.74 cm cell was used for all the width and strength measurements, except the  $2.3\mu\text{m}$  CO band. The sample cell in this case was the entire input optic. A sapphire window was placed between the input optic and the entrance slit. The cell thus created was 300 cm long.

### 2.2.4 Entrance Optics

An image of the source 2.8 cm high was formed on the entrance window. The light beam diverges from this point to a diagonal mirror 8 cm x 6 cm approximately 100 cm away placed just beyond the entrance slit. The beam is diverted by the diagonal mirror to a 66.6 cm focal length spherical mirror 115 cm in diameter. The beam is imaged by the spherical mirror on the entrance slit one meter away. The image height on the entrance slit is 1.4 cm. The aperture ratio of the beam at this point is F/10.



### 2.2.5 Slits

The entrance and exit slits are identical and were made in the U of M. Physics shop (Fig. 4). The slits are curved and ground to fit as 8.5 inch diameter circle. The inside portions of the slits are fixed in place and were adjusted on installation to fit an image circle. The outside sections of the slits are ground to a matching circle and mounted on parallel leaf springs. The slit rest position is open by about 1 mm. The differential screw which pushed on the moveable jaw changes the slit width  $50\mu\text{m}$  per revolution. The total slit height is 3.125 inches. However, the image height used for double pass was about 0.625 inches. Vacuum feed through manipulators were installed in the wall of the main tank to permit adjustment of the slits while the instrument was evacuated. The micrometer screw could be turned with the manipulator and then completely disengaged from the slit mechanism.

### 2.2.6 Basic Instrument

The slits are positioned at the focus of the 1.83m main mirror. The mirror is located at the opposite end of the 80 inch vacuum tank. The 16 inch diameter main mirror is secured on three horizontally adjustable mounts. The mounts are located at  $0^\circ$ ,  $120^\circ$ , and  $240^\circ$  with separate access holes for each adjustment. By the proper use of the adjustments the mirror can be tilted side to side, up and down, or displaced front to back.

The light from the entrance slit diverges at  $F/10$  and passes through the input baffle. The light continues to diverge and strikes the upper right hand corner of the main mirror. The light is collimated by the mirror and directed toward the grating. The original circular bundle of light is apertured by the grating and diffracted into a series of rectangular bundles and returned to the lower left hand corner of the large mirror.

The main mirror focuses the beams into an array of images. A few of the beams strike the pass mirror located directly in front of the lower half of the slit. The rays are directed behind the grating and come to a focus at the center line of the instrument. A baffle located at the focus helps to eliminate the stray light. A slit located at this point would be preferred. If the chopper could be located at this point most of the stray light would not be modulated and hence undetected.

The light diverges again and is reflected by the second pass mirror in front of the lower half of the entrance slit. The light diverges towards the lower right half of the large mirror. It is again collimated and directed towards the grating. The total optical retardation is doubled and the theoretical resolution is increased by a factor of two.

The diffracted beam is directed towards the upper left quadrant of the large mirror. The beam is focused on the top half of the exit slit. The beam at this point has traveled 327 cm in the entrance optics and 1412 cm in the basic instrument for a total of 1739 cm.

## 2. 2. 7 Gratings

The gratings used in the instrument were supplied by Bausch and Lomb and have a total area of 135mm x 220mm. The ruled area is 128mm x 208mm. The grating mount was designed for a Jarrell-Ash grating, 80mm x 190mm. In order to accommodate the larger grating, an adaptor was designed and it was necessary to have the back corners of grating blank removed (Fig. 6) to prevent aperturing the input beam.

The grating holder is mounted in two precision ball bearings and the drive shaft extends through the vacuum wall.

The complete grating drive system mounts on top of the main

frame outside the vacuum (Fig. 7). The drive consists of a variable speed gear box, a counter, a precision slide, an optical flat, and a grating pivot arm. Adjustments are provided for the arm position, arm length, and angular orientation of the optical flat. The adjustments are used to obtain a linear relation between the counter reading and wavelength.

The theoretical resolution depends on the maximum optical retardation. The optical retardation is a function of grating size and the blaze angle. The steeper the blaze angle, the greater the retardation.

- 1) The  $16\mu\text{m}$  grating has a blaze angle of  $28^{\circ}41'$  and the optical retardation =  $2 \times 208\text{mm} \times \sin 28^{\circ}41' = 198\text{mm}$ . Resolution =  $1/\text{retardation} = .0515 \text{ cm}^{-1}$ .

If the instrument is double passed the theoretical resolution =  $.026 \text{ cm}^{-1}$   
the best measured resolution =  $0.05 \text{ cm}^{-1}$ .

- 2) The  $4.0\mu\text{m}$  grating has a blaze angle of  $17^{\circ}27'$ .

$$V = 1/2 \times 208 \times \sin 17^{\circ}27' = 1/12.48 \text{ cm} = .083 \text{ cm}^{-1}$$

$$V, \text{ double pass} = 0.042 \text{ cm}^{-1}$$

The best measured resolution  $0.08 \text{ cm}^{-1}$  at  $4.3\mu\text{m}$

$0.12 \text{ cm}^{-1}$  at  $2.3\mu\text{m}$

#### 2.2.8 Exit Optics

The beam entering the exit optic is F/11 and diverges to just fit a rectangular image of the grating inside the 115mm dia. 37 cm focal length mirror located one meter from the exit slit. A new image is formed 60 cm away. The focused beam is intercepted by a diagonal mirror 55 cm away. The image is formed at one focus of the elliptical mirror,  $M_8$ . The focal distances for  $M_8$  are 60 cm and 9.5 cm. The image height at the first focus is 8.4mm and at the second focus, 1.33mm. A very small diagonal mirror  $M_9$ , about

2mm square mounted on a diagonal strip is placed at the second focus. The image formed is also at the first focus of the elliptical mirror,  $M_{10}$ , a distance of 14 cm. The second image is formed at 21 cm and falls directly on the detector flake. The final image height is 2.0mm. The path length through the exit optics is 264.5 cm for a total path from source to detector of 2003.5 cm.

Manipulators to adjust both elliptical mirrors are brought through the vacuum walls to the outside. In normal operation there is no need to adjust  $M_8$ , but  $M_{10}$  which focuses the image on the flake is normally adjusted prior to each daily run.

### 2.2.9 Detector

The Cu: Ge detector purchased from Texas Instruments and used for the  $15\mu\text{m CO}_2$  study had a sensitive area 2mm x 0.25mm. The flake was mounted on a brass finger which in turn was mounted on the liquid helium container. The dewar was designed so that the liquid helium is surrounded by a liquid nitrogen jacket. A copper shield is attached to the nitrogen jacket.

In the preferred dewar design, the copper shield completely surrounds the brass finger and the interference filter used as an order sorter is mounted on the copper shield. The dewar window was made of potassium bromide.

In the case of the original dewar, the brass finger protruded through the nitrogen shield. The interference filter was mounted on the brass finger and cooled to liquid helium temperature. There are two problems with this design: (1) the flake temperature is affected by the instrument temperature, which causes the sensitivity to drift, and (2) the interference filter after being repeatedly heated and cooled begins to separate.

The indium antimonide detector used for the  $4.3\mu\text{m}$  and  $4.6\mu\text{m}$

studies was also purchased from Texas Instruments and mounted in an IR-15 dewar. The dewar was of the newer design, but the inner container was filled with liquid nitrogen.

The lead sulfide detector used for 2.3 $\mu$ m studies was an Eastman detector. The dewar was an IR-10 similar in design, but having a smaller liquid capacity. The flake was cooled to the dry ice temperature of -78°C. A slurry of ethyl alcohol and dry ice was used. The order sorting interference filter was mounted externally on the window. In this spectral region the window radiation was insignificant.

### 3.0 Data Recording System

The outputs of the detectors are electrical signals proportional to the total number of photons falling on the flake. The input radiation is chopped at 90Hz and the detector output signal is a 90Hz square wave.

The detector impedance is determined by the average number of photons striking the surface. The impedance increases as the photon flux is reduced and the change in voltage corresponding to a change in photons increases. In other words the sensitivity or  $D^*$  of the detector increases.

The Cu: Ge detector is sensitive out to 30 $\mu$ m. By reducing the stray radiation falling on the flake, the sensitivity was very much improved. Originally, the interference filter was placed on the detector window. However, by moving the filter to the helium cooled finger, the signal to noise increased by more than a factor of two.

The bias arrangement for each detector was slightly different. The bias arrangements are shown in Fig. 8. In the case of the Cu: Ge detector, the input resistance was made equal to the detector impedance, which varied depending on the filter used.

Considerable experimentation was done with the InSb detector to find the optimum bias. The bias voltage, measured at the input to the amplifier was set at -6mV. It was found that the bias was a critical function of the temperature of the spectrometer. A temperature change of 1°C produced a change in bias of 1.2mV. A change of ±2mV would increase the signal to noise by a factor of two.

### 3.1 Pre-Amplifier

The pre-amplifier used with the Cu: Ge detector was an FET amplifier designed by C. B. Arnold of the Infrared Laboratory. The pre-amp used with the InSb was an Ithaco Model 112 which has an input impedance of 1000 meg ohms, a gain of 100, and an output impedance of 100 ohms. The pre-amp was located as close to the detector as possible.

### 3.2 Phase-Lock Amplifier

The pre-amp output is coupled by co-ax cable to the Princeton Applied Research Model 120 phase lock amplifier. The phase lock reference signal is derived from the chopper. The amplifier attenuators are used to adjust the system gain. A total adjustment of 1000 is possible by using a 500 to 1 attenuator and a 2 to 1 gain control. The zero can be set to any position ± one full scale reading. The output filter can be set for time constants from one milli-second to 30 seconds. The data was always recorded at 11 seconds per resolution element and the amplifier time constant was generally set at one second. If the signal to noise was less than 20 to 1 the recording was made with a 2 second time constant. The signal to noise of many scans was better than 200 to 1 and a time constant of 0.1 seconds was used.

### 3.3 Analog Chart Recorder, Leeds & Northrup Speed-O-Max Type G

The recorder provided the immediate visual output signal.

Normally, the gain of the phase-lock amplifier was set so that the recorder read full scale with no gas sample in the cell. A recording under this condition was used to indicate the system noise. If the detector was being adjusted, the recorder meter was used as an adjustment indicator. A noise record was made prior to each daily run to indicate correct operation of the system.

### 3.4 Integrating Voltmeter - Hewlett-Packard DY 2401C

The voltmeter was very well suited to the data collection requirements. Basically, the instrument consists of a highly accurate and linear voltage to frequency converter, a frequency counter, and a crystal oscillator. The signal voltage is applied to the voltage to frequency converter. The counter converts the pulses from the frequency converter for a specific time period determined by the crystal oscillator. At the end of the counting period, the count is displayed on the front panel and stored in the shift register.

The features that make the Hp 2401C desirable for the spectrometer application are:

- 1) High accuracy: - example, a resolution of  $1\mu\text{v}$  on the 0.1 volt scale.
- 2) Read out compatibility: - the voltmeter was directly interfaced with an H. P. 2526 card coupler. The card coupler drove an IBM 525 summary punch.
- 3) External frequency standard provision:

The 100 KHz crystal oscillator is the internal frequency standard and has a stability of  $\pm 2/10^6$  parts per week. If an external standard is used, it can be directly substituted through a switch and a connector in the rear.

We elected to substitute a laboratory oscillator for the internal frequency standard. The stability of the laboratory oscillator was  $\pm 2/10^4$  parts per week. However, the frequency could be set to any desired value. The

frequency determines the integration time. Hence, the integration time could be precisely matched to the encode pulse period.

The poor stability of the laboratory oscillator made the last voltmeter digit unusable. However, this was unimportant since the desired accuracy was  $1/10^3$ .

The time between encode pulses was determined by the grating drive and the spacing between the slits in the encoding wheel. The nominal encoding time for the two scan speeds used was 2.2 seconds and 6.6 seconds. Originally the integration time was set almost equal to the encode time, but it was soon determined that the mechanical spacing of the slits in the encode wheel varied slightly. If the encode time was less than the integration time, the storage register would be empty when the encode pulse was received and a zero value would be printed. The problem was avoided by reducing the integration time to 2.150 seconds and 6.550 seconds.

### 3.5 Digitizing Signals

The encoding and storage of the data will be described by referring to the block diagram (Fig. 9). The output of the phase-lock amplifier is a D. C. signal which varies from 0 to  $\pm 5$  volts. The signal can be off-set from zero to full scale in either polarity. The usual procedure was to use a 5% off-set from zero and set the gain of the L & N recorder so that full scale on the recorder corresponded to full scale on the phase-lock amplifier.

The output of the phase-lock amplifier was applied through a divider to the integrating voltmeter. The integrating voltmeter was set on the 100-volt scale. The divider was set so that full scale on the L & N recorder corresponded to 9.99 volts on the integrating voltmeter. The actual input voltage was  $9.99/2.150 = 4.65$  volts. The difference is because the instrument



was calibrated for an integration time of one second rather than 2.150 seconds.

The encoding pulses are derived from the photo cells associated with the encoding wheel attached to the grating drive motor shaft. The first encode pulse received by the voltmeter clears the shift register and the counter. The counter then begins to count the voltage to frequency converter pulses. The counting period is determined by counting a specified number of reference oscillator pulses. At the end of the counting period the accumulated count corresponding to the integral of the voltage during the counting period is transferred to the shift register and displayed on the front panel.

The next encode pulse transfers the contents of the shift register to the card coupler. The three digits corresponding to 9.99 volts on the 100-volt scale are transferred to the IBM 526 Summary Punch.

The pulse shaper also sends pulses corresponding to the encode pulse and the revolution counting pulse to the IBM summary punch. The encode is wired to punch an "\*" and the revolution pulse punches a "-". These pulses are used to separate the data words and identify a complete revolution of the encoding wheel. Each card contains 80 lines or 20 data points. Five cards are required for one revolution of the grating drive screw, a scan of approximately  $1 \text{ cm}^{-1}$ .

The grating drive moved slowly enough so that it was quite easy to start taking data at any selected point. The practice followed was to start taking data one point before the revolution mark. The revolution counter number was noted on the scan identification card. Each succeeding data point corresponded to 0.1 counter numbers. The computer programs converted the counter numbers to wave numbers.

### 3.6 Computer Outputs

The data to be used for line strength and width measurements must be normalized. The usual procedure is to make a 100% transmission scan. The 100% line quite often fluctuates in amplitude due to the order sorting interference filter. The 0% transmission was usually a constant value dependent on the amplifier gain settings. The 0% transmission line was originally established by measuring the transmission at the center of completely absorbing lines. This value should be the same as that obtained by blocking the beam. Hence, the 0% line was established daily by blocking the beam and running two cards to provide one average value.

The usual procedure was to tabulate the transmission data and also have it plotted by a Cal-Comp plotter associated with the computer. The examples of data given in this report are computer output plots.

### 4.0 Gas Handling System

The gas handling equipment is best described by referring to the diagram (Fig. 10). The purpose of the system shown was to place known quantities of gas in the sample cell or in the main frame of the spectrometer. The original thought was that data would be taken using several sample cell lengths. Hence, the vacuum disconnect between two valves. Actually, all the data was taken with two cells or with gas in the main frame.

The manifold was provided with three separate pressure gages. The mercury monometer was used to indicate the main frame pressure when the instrument was being back-filled with nitrogen or when rough pumping was in process. The thermocouple was used to monitor the vacuum in the manifold before filling with any gas. The Baratron pressure gage was used to measure the amount of gas placed in the sample cell.

The Baratron gage proved to be very useful. The internal bridge circuit allowed the operator to set the bridge at the desired pressure and then let gas into the manifold until the exact pressure was reached. As the bridge balance point was approached the meter was switched to a more and more sensitive scale. Thus, an almost exact setting of the pressure could be obtained. The Baratron gage head is a differential diaphragm which forms two legs of an a. c. bridge. The pressure to be measured is placed on one side of the diaphragm and the reference pressure on the opposite side. In our application, the reference side was always connected directly to the vacuum line.

The task of filling the sample cell with a known mixture was not as straight forward as we originally expected. It was expected that the gases would be mixed in the manifold and valved into the sample cell. The procedure was satisfactory at pressures less than 10 milli-torr. However, at the higher pressures the mixing time increased rapidly to the order of hours.

The procedure was altered. First, the volume ratio between the sample cell and the manifold was precisely determined. The gas to be studied was placed in the manifold with the valve to the sample cell open. The pressure was measured with the Baratron and the valve between the sample and the manifold was closed. The gas in the manifold was then pumped out to a few microns as measured on the thermocouple gage.

Knowing the volume ratio between the manifold and the sample cell, and how much gas was in the sample cell, the amount of gas to be placed in the sample cell was calculated. The broadening gas was placed in the manifold. The Baratron bridge was set to the calculated mixed pressure. The pressure in the manifold, at this point, was higher than the cell pressure. Opening the valve between the manifold and the sample cell allowed the broadening gas

to flow from the manifold into the sample cell. Pressure equalization was noted by observing the Baratron meter. When the pressure equalized, the valve between the cell and the manifold was closed.

Since the broadening gas forces the original gas sample into the ends of the cell there is no chance of a reverse flow of the original gas before the valve is closed. Even though the gas in the sample cell may not be completely mixed, the total pressure is known and the amount of sample gas in the optical path is known. No difference was ever detected between the 8.74 cm samples measured shortly after mixing and those which had stood for one day.

#### 4.1 Purge Gas

The nitrogen gas used for back-filling the spectrometer was the boil off from a large liquid nitrogen storage dewar. The same gas was used to broaden the CO<sub>2</sub> and CO samples, as well as purge the portions of the optical path at atmospheric pressure.

The total atmospheric pressure path was about 17 cm. The 9.0 cm from the source to the lens was purged with argon. The 6.0 cm from the lens to the cell and 2.0 cm from cell to the spectrometer window were purged with nitrogen. As mentioned in Section 2.2.2 both ends of the cell were wrapped with polyethylene and taped to the spectrometer and chopper housing. A purge of 20 liters per minute was used to completely eliminate CO<sub>2</sub> from the path. The system was quite effective since no lines could be detected in the strongest part of the 4.3 $\mu$ m CO<sub>2</sub> band.

#### 5.0 Temperature Control

##### 5.1 Room Heaters

In order to maintain the instrument optical alignment it was

required that the room temperature be very carefully controlled. The room was equipped with four thermostatically controlled 3Kw strip heaters. One heater located along each wall. Three of the thermostats were bi-metal strips and the other heater was controlled by a mercury thermometer controller accurate to  $0.1^{\circ}\text{C}$ . The thermometer controller operated a relay which in turn operated the heater. During some of the later scans it was found that the relays introduced noise pulses into the data. The mercury controller was removed and a Variac was used to power the heater. The Variac setting was continually changed during the day depending on the amount of external heating. For example, if the day was overcast with heavy clouds very little control was required.

The heaters alone were used for control in the winter, but during the rest of the year air-conditioning was required. There were two air-conditioners in the room, (10,000 BTU and 20,000 BTU) and both were required for the warmest days. For most of the year the larger air-conditioner was more than adequate. The room was controlled by using the larger air-conditioner in conjunction with the Variac controlled heater.

The room temperature as measured by a mercury thermometer near the spectrometer was kept to  $\pm 1^{\circ}\text{C}$  for most of the  $15\mu\text{m CO}_2$  data. Control to  $\pm 0.5^{\circ}\text{C}$  was aimed for during the remainder of the data taking. Even though it was possible to maintain close control of the reference thermometer, the spectrometer temperature usually drifted during the day. The source and the electronics were turned off at night and the temperature was controlled by bi-metal heaters which allowed the whole room to drop about  $2^{\circ}\text{C}$  in temperature. Also, the source radiation raised parts of the spectrometer above room temperature. The critical sensitivity to temperature was observed only at the shorter wavelengths.

## 6.0 Optical Alignment and Set-up

In order to change the grating it was necessary to remove the input optics, exit optics, the front flange, and the baffles. The main frame of the instrument was never moved and neither the slits nor the pass mirrors ever required adjustment. On one occasion the large mirror was adjusted in order to check the focus at the exit slit.

### 6.1 Main Mirror Adjustment

The main mirror is mounted on three adjustable pads at  $0^\circ$ ,  $120^\circ$ , and  $240^\circ$ . The adjustments are accessible through openings in the rear cover flange. The mirror is adjusted with respect to the input and exit slits by first rotating the grating to  $90^\circ$  so that no light strikes the grating. Threads were used to mark the center of both slits. A He-Ne laser was adjusted so that the beam crossed the thread on the exit slit. The angular position of the mirror was then adjusted.

The grating was turned to the  $0^\circ$  position equivalent to the zero order. The entrance slit was illuminated with a mercury lamp. The second pass light was blocked behind the grating. The grating was tilted back and forth so that the image fell on the exit slit. The large mirror was then adjusted front to back to obtain the best focus. The mirror was then completely adjusted.

### 6.2 Grating Adjustment

The grating was turned to a position very close to the blaze angle. The threads across the entrance and exit slits were moved up 1/2 inch. The He-Ne laser was then adjusted so that the beam intersected the thread across the input and struck the large mirror slightly above and to the right of center and the reflected beam struck the center of the grating. If the grating was set at blaze a pattern similar to that shown in Figure 12 would be seen. The output beam intersects the thread across the exit slit.

If the above pattern was not seen the second pass light was blocked. The grating was rotated until the order closest to the blaze was positioned such that the diffracted beam was spaced as far to the left of center as the input beam was to the right. The reflection was made symmetrical about the horizontal center line by adjusting the grating tilt. The diffracted beam should define a line passing through the input beam. If this was not true, the grating level was adjusted by means of the pivot screw.

The second pass was unblocked and the diffraction patterns from the 1st and 2nd passés formed a cross passing through the input beams. A line drawn through the off blaze orders formed lines parallel to the horizontal center line.

### 6.3 Baffles

The primary purpose of the baffles was to reduce the stray light to a minimum. A secondary purpose was to keep any 1st pass light from entering the exit slit. After the baffles were fastened in place a final adjustment was made by taping optical black tape along the baffle edge.

The entrance slit was illuminated with a mercury light filtered to the green line and the grating was observed through the exit slit. The mask was adjusted so that no first pass light could be seen on the grating. If any were present it would form a bright band at the top edge of the grating. As a final check, the first pass and second pass images were located with tissue paper at the exit slit.

The mask used to eliminate the direct ray from the entrance to the large mirror to the exit slit was a small piece of velvet cloth suspended by means of threads in front of the mirror.

#### 6.4 Slit Alignment

The slit alignment was checked by placing a mercury lamp at the entrance slit and observing the exit slit as the grating was slowly scanned. If the alignment were perfect the image would appear and disappear simultaneously along the entire length. This appeared to be the case when the slits were set at  $200\mu\text{m}$ . However, when the slits were set at  $50\mu\text{m}$  a slight "walking" of the image could be detected. The amount seemed to be a function of room temperature and the maximum was estimated to be  $5\mu\text{m}$ .

#### 6.5 Input and Exit Optics Adjustment

Following the slit alignment check the input and exit optics were re-assembled. A mercury arc lamp with a green line filter was placed at the source position. The grating was adjusted to the order closest to the blaze. There was enough light so that every mirror in the system could be checked to see if it was properly filled with light. During the first check it was found that the exit sphere was aperturing part of the grating image. The fault was corrected by re-soldering the exit mounting flange.

The mercury lamp was moved to exit and the image located at the input. The mirrors were again checked and the correct source position located.

The carbon source was located in position and the grating placed at blaze with the slits open to  $400\mu\text{m}$ . The output mirrors were then adjusted to place the white light image in the center of the detector mounting hole.

#### 6.6 Image Adjustment

The final image adjustment was done with the detector installed by observing the analog output. Usually the first detectable signal was quite small compared to the ultimate signal. The beam is very fast at the output



F/1.4 and a very small error in the vertical position of the beam severely attenuates the signal.

The adjustment procedure was to scan the image across the detector in both the x and y direction using the adjustments on the bottom ellipse. After locating the maximum signal position the z adjustment was moved slightly. The procedure was continued until the optimum x, y and z position was located. It was necessary to rotate the detector since the detector sensitive area is 2mm x 0.25mm.

#### 6.7 Slit Width Adjustment

The slit width is a compromise between resolution and signal to noise ratio. A resolution equal to twice the theoretical value was readily obtained. However, a large sacrifice in signal to noise was required for improvements beyond this value.

Our original procedure for determining the slit width was to measure the half-width of an isolated line using various slit settings. As the slit width was decreased both the amplitude and line width would initially decrease. The slit width at which the line width no longer decreases was noted. The usual procedure was to open the slits slightly after the best resolution position was reached.

An alternative resolution test was devised for the 15 $\mu$ m band. The Q-branch of band (010:1-100:0) at 720.8cm<sup>-1</sup> was scanned and compared to theoretical scans of the same band using various resolutions (Fig. 13). The instrument resolution was assumed to be equal to the best match between the theoretical and measured scans.

The resolution which we were able to obtain with 200 $\mu$ m slits varied from 0.048 cm<sup>-1</sup> to 0.060 cm<sup>-1</sup>, depending on the temperature gradients in the spectrometer. The most common value was 0.052 cm<sup>-1</sup>.

## 7.0 Operating Procedures

The  $15\mu\text{m}$   $\text{CO}_2$  measurements required the helium cooled Cu: Ge detector. The filling system available required that the detector be removed from the spectrometer to be filled.

The spectrometer was normally left under vacuum. Hence, the first step was to valve off the vacuum pump and back fill the instrument with nitrogen gas. The detector was removed and if it had not been used the previous day, it was filled with liquid nitrogen to pre-cool the dewar. The dewar was filled with helium and returned to the spectrometer. The spectrometer was re-pumped to a pressure of less than 10 micro-torr. If it was less than one hour from back-filling to re-pumping, the original vacuum could be restored in about one-half hour.

During the time that the vacuum was being restored the following items were checked.

1. Argon trap filled with solid  $\text{CO}_2$ .
2. Argon flow turned on.
3. Source cooling water turned on.
4. Source secondary current adjusted to 250 amps.
5. Chopper - on.
6. Electronics - on.
7. Final image adjusted in x-y plane for maximum signal.
8. Integrating time checked for 5 minutes and set equal to  $2.150 \pm .001$  seconds.
9. Test scan made to check sensitivity and signal to noise ratio.
10. Check spectrometer vacuum, if o. k. - start background scan.

## 7.1 Data Collection

Prior to collecting data, survey scans of the bands to be studied were made and counter numbers recorded on analog plots. Using the survey scans, areas to be studied were selected. The data collecting procedure was to begin each scan with an integral revolution of the grating drive screw. The counter number was marked on the scan identification card.

The scan start procedure was as follows:

1. Locate area of maximum signal and set PAR amplifier gain. Integrating voltmeter should read near to but less than 9.99 volts.
2. Set grating drive at number less than starting point.
3. Set scan speed equal to  $0.3 \text{ cm}^{-1}/\text{minute}$ .
4. Turn on L & N recorder and lower pen.
5. Set PAR filter to 1 second or less.
6. Watch revolution counter and when correct counter number is reached start card punch.
7. Verify that card punch started at correct point.
8. Record room temperatures, gas cell temperatures, and gas cell pressures.
9. Monitor room temperatures at regular intervals and modify either air-conditioner or Variac controlled wall heat if temperature varies more than  $0.5^{\circ}\text{C}$ .

### NOTE:

1. Whenever data was taken on line widths and strengths, background scans were made before and after recording the data.
2. Zero percent transmission scans were made at the end of the day

3. If the data was taken for line position measurements, the gas was sometimes placed in the main frame to obtain a longer path and lower pressure.
4. The InSb and PbS detectors, which required liquid N<sub>2</sub> and solid CO<sub>2</sub> for cooling, were filled in place.
5. The isotope enriched samples had to be handled with special care. We attempted to retrieve the sample after each usage by trapping it back into the original container by liquid nitrogen cooling.

#### 8.0 Data and Measurements

The data obtained are summarized in Table 1. During the course of the investigations more than 700 spectra were obtained. At least six separate spectral regions in each band were studied by self-broadening and nitrogen broadening. The cell length used for all the studies with the exception of the 2.3 $\mu$ m band of CO was 8.74 centimeters. The 2.3 $\mu$ m band data was taken with a 300 centimeter cell. The frequency position measurements utilized the 20 meter path through the instrument. In the case of the isotope measurements, the enriched isotope sample was placed in the cell and ordinary CO<sub>2</sub> was placed in the 20 meter path for calibration purposes. The nominal temperature for all the measurements was 26°C.

Examples of typical spectra are given in Figures 14-39. The typical spectra include samples from each spectral band as well as samples to illustrate the noise, resolution, and background limitations.

All of the spectra are stored on IBM cards. There are 20 spectral points per card and the points are approximately 0.01 wave-numbers apart. Copies of the IBM cards for any spectrum will be available upon request until March 1, 1973.

### 8.1 Line Position Measurements ( $15\mu\text{m CO}_2$ )

Carbon dioxide  $15\mu\text{m}$  band line position measurements were made covering the entire band from  $12\mu\text{m}$  to  $18\mu\text{m}$ . The measurements represent a significant improvement over existing data. The data has been carefully studied and analyzed by Roland Drayson<sup>3</sup> and is the subject of a paper and report.

Examples of the data are given in Figures 14-23.

### 8.2 Isotope Measurements ( $15\mu\text{m CO}_2$ )

Isotope enriched carbon dioxide gas samples were measured in the  $15\mu\text{m}$  band. The samples obtained were enriched in  $^{13}\text{C}$ ,  $^{18}\text{O}$ , and  $^{17}\text{O}$ . Many spectra were taken of each sample.

Examples of  $^{13}\text{C}$  are given in Figures 24-28.

Examples of  $^{18}\text{O}$  are given in Figures 29-30.

Examples of  $^{17}\text{O}$  is given in Figure 31.

It should be noted that  $^{18}\text{O}$  contained about 50%  $^{16}\text{O}$  which produced  $^{12}\text{C}^{16}\text{O}^{18}\text{O}$ ,  $^{12}\text{C}^{18}\text{O}^{18}\text{O}$ , and  $^{12}\text{C}^{16}\text{O}^{16}\text{O}$  in about equal strengths. The case for the  $^{17}\text{O}$  sample was even more confused since  $^{17}\text{O}$  is rather rare and is contaminated by large amounts of both  $^{16}\text{O}$  and  $^{18}\text{O}$ . The isotope bands are being analyzed by James B. Russell and will be the subject of his doctoral thesis.

### 8.3 Carbon Dioxide $4.3\mu\text{m}$ Band

The indium antimonide liquid nitrogen cooled detector was used to study this band. The fourth order of the  $16\mu\text{m}$  blazed grating was isolated with an optical coating laboratory interference filter. The study was to determine the widths and strengths of individual lines. The cell used was 8.74 cm long. Many self broadened and nitrogen broadened scans were made.

Examples of the data are given in Figures 32-35.

Roland Drayson has made a preliminary study of the data and plans to continue with a detailed study.

#### 8.4 Carbon Monoxide 4.6 $\mu$ m Band

The band was studied using two separate gratings. The first grating was blazed at 16 $\mu$ m and used in the fourth order. However, the order sorting interference filter was not satisfactory for the entire band.

The second grating was blazed at 4.0 $\mu$ m and used in the first order. The P branch of the band was measured with this grating.

The individual lines in the band are sufficiently far apart so that the reference was obtained from the absorption data. A single 100% transmission scan corresponding to the region to be studied was required for a given amplifier gain setting.

All the data in the study were taken using the 8.74 cm cell. The selected spectral lines were studied by self broadening and nitrogen broadening.

Samples of the data are shown in Figures 36-38.

The data is now being analyzed by Rao Tallamraju and it is expected that this will be the subject of his doctoral thesis.

#### 8.5 Carbon Monoxide 2.3 $\mu$ m Band

The band was studied with the grating blazed at 4.0 $\mu$ m and filtered for the second order. The band was completely isolated by a narrow band interference filter obtained from Optical Coating Laboratories. The detector used was a lead sulfide element cooled to -78<sup>o</sup> with dry ice in ethyl alcohol.

The cell used was made from the entrance optics by placing a window between the entrance optics flange and the spectrometer main frame. The total path length was 3.0 meters. The cell was actually one meter from the

input window to a diagonal mirror and another meter from the diagonal mirror to the spherical mirror. The last meter was folded back to the entrance slit.

The fact that the light passed once through one leg and twice through the other leg created a problem in the nitrogen broadening studies. The nitrogen and carbon monoxide had to be completely mixed. Otherwise, there would be more carbon monoxide in one leg than the other. The procedure used was to add nitrogen at the end of the day and let it mix over night. Spectra were then made of all lines to be studied with the mixture. The mixture would be changed and allowed to stand overnight before taking additional data.

An example of the data is given in Figure 39.

## References

1. L. D. Kaplan, J. Optic. Soc. Am., 49, 1004 (1959).
2. S. R. Drayson, Space Research, XI, 585, (1971).
3. S. R. Drayson, To be submitted for publication.



Table 1

## DATA SUMMARY

<u>Scan No.</u>	<u>Band</u>	<u>Frequency</u> <u>cm<sup>-1</sup></u>	<u>Cell</u>	<u>Pressure</u>	<u>Purpose</u>
1-22					Instrument testing
23-51	15 $\mu$ m CO <sub>2</sub>	711-715	8.74cm	5mm - 640mm	Line intensity by self broadening
52-63	"	696-701	"	" "	"
64-74	"	672-677	"	" "	"
75-101					Instrument testing re-adjust To eliminate stray light.
102-125	15 $\mu$ m CO <sub>2</sub>	672-677	8.74cm	5mm - 320mm	Line intensity by self broadening
126-145	"	709-715	"	5mm - 640mm	"
146-162	"	696-701	"	" "	"
163-169	"	630-711	"	30mm - 100mm	Frequency position
170-217	"	541-831	20meters	2mm - 400mm	"
218-224	"	614-670	8.74cm	0.2mm - 400mm	"
225-244	15 $\mu$ m CO <sub>2</sub> (C <sub>13</sub> isotope)	713-574	"	9.0mm - 400mm	"
245-248	"	680-722	8.74cm/20meters (C <sub>12</sub> in 20 meter tank and C <sub>13</sub> in 8.74 cm cell)	150mm - 300mm	"

DATA SUMMARY (cont'd)

<u>Scan No.</u>	<u>Band</u>	<u>Frequency</u> cm <sup>-1</sup>	<u>Cell</u>	<u>Pressure</u>	<u>Purpose</u>
249-260	15μm CO <sub>2</sub> (O <sub>18</sub> isotope enriched)	595-722	8.74cm/20meters	19mm - 64mm	Frequency position
261-294	15μm CO <sub>2</sub> (O <sub>18</sub> & O <sub>17</sub> enriched)	576-755	8.74cm/20meters	15mm - 300mm	"
295-310	15μm CO <sub>2</sub> (C <sub>13</sub> enriched)	570-728	8.74cm	12mm - 300mm	"
311-314	4.6μm CO				Instrument test
315-323	"	2224-2230	8.74cm	10mm - 640mm	Line intensity self broadening
324-335	"	2145-2148	"	5mm - 640mm	"
336-342	"	2135-2145	"	5mm - 640mm	"
343-349	"	2058-2065	"	20mm - 320mm	"
350-404	4.3μm CO <sub>2</sub>	2345-2352	"	0.2mm - 160mm	"
405-411	"	2301-2305	"	0.3mm - 160mm	"
412-434	"	2378-2380	"	0.3mm - 320mm	"
435-446	"	2378-2380	"	0.3mm - 20mm	Line intensity by nitrogen broadening
447-454	4.6μm CO	2224-2230	"	10mm - 80mm	"
455-481	"	2145-2148	"	10mm	"

DATA SUMMARY (cont'd)

<u>Scan No.</u>	<u>Band</u>	<u>Frequency</u> cm <sup>-1</sup>	<u>Cell</u>	<u>Pressure</u>	<u>Purpose</u>
482-508	4.6μm CO	2180-2185	8.74cm	2.5mm - 40mm	Line intensity by nitrogen broadening
509-516	"	2145-2150	"	5.0mm	"
517-523	"	2055-2060	"	10mm - 640mm	Line intensity by self broadening
524-532	"	2055-2060	"	10mm	Line intensity by nitrogen broadening
533-542	4.3μm CO <sub>2</sub>	2378-2380	"	5mm	"
543-548	"	2390-2392	"	200mm - 700mm	Line intensity by self broadening
549-560					Instrument testing
561-572	15μm CO <sub>2</sub>	696-701	"	5mm	Line intensity by nitrogen broadening
573-586	"	599-602	"	20mm - 40mm	"
587-595	4.6μm CO	2090-2095	"	5mm - 640mm	Line intensity by self broadening
596-613	"	2090-2095	"	1.5mm	"
614-752	2.3μm CO	4332-4336 4310-4313 4283-4287 4255-4276 4242-4246 4229-4234 4193-4197 4152-4156	300cm	2.5mm - 640mm	Line intensity by self-broadening and nitrogen broadening

42

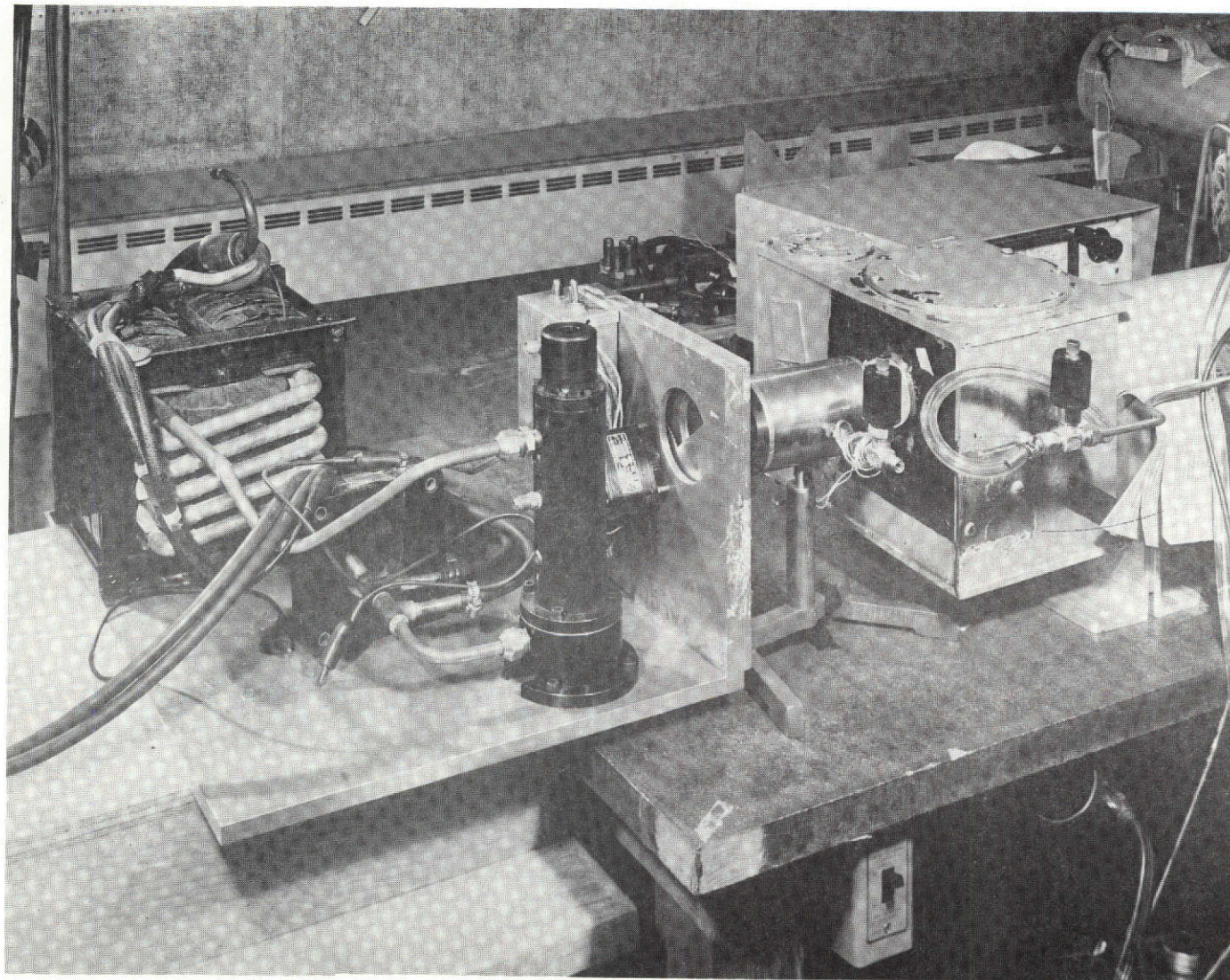


Fig. 1. Graphite Rod Source

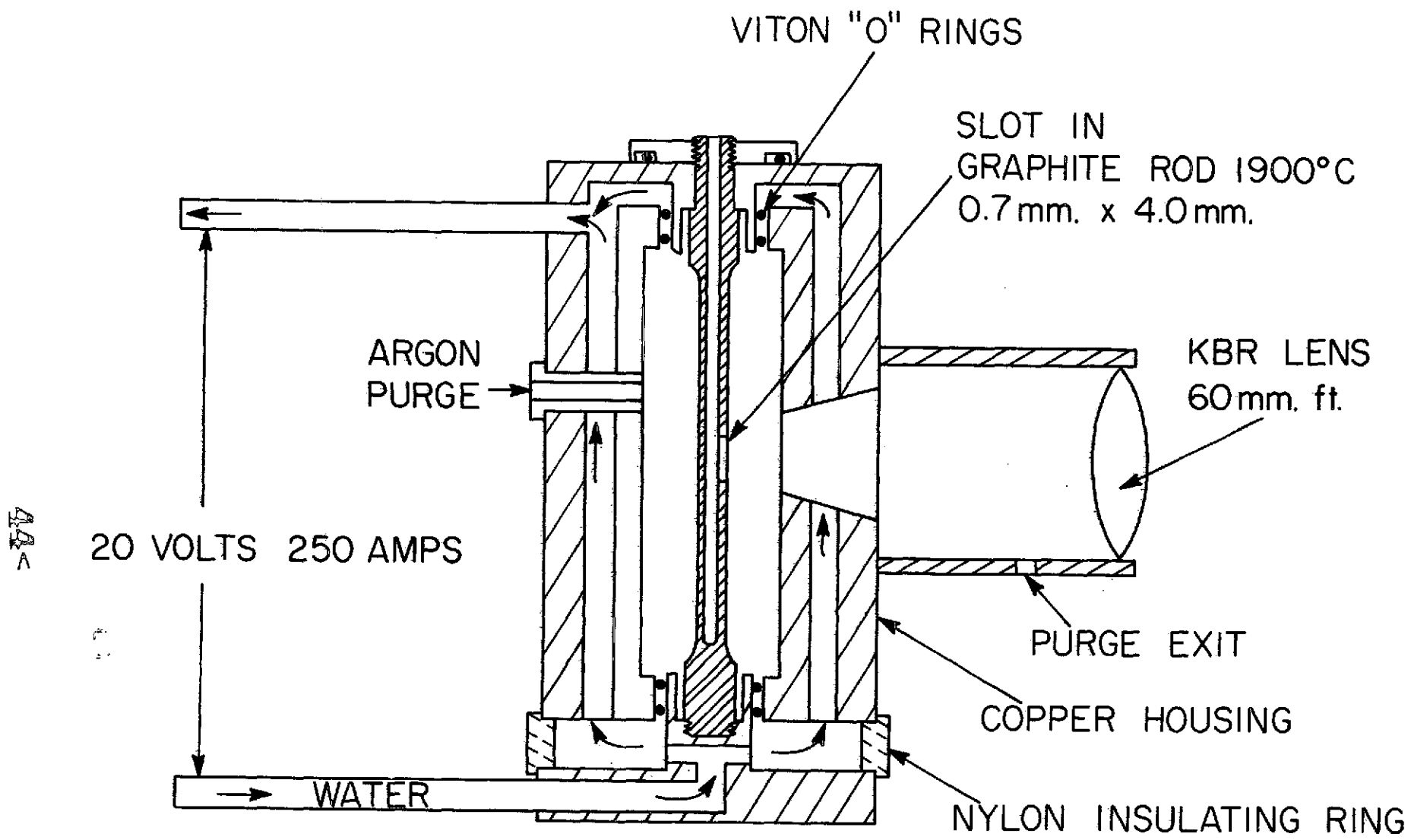


Fig. 2. Cross-sectional diagram of graphite source.

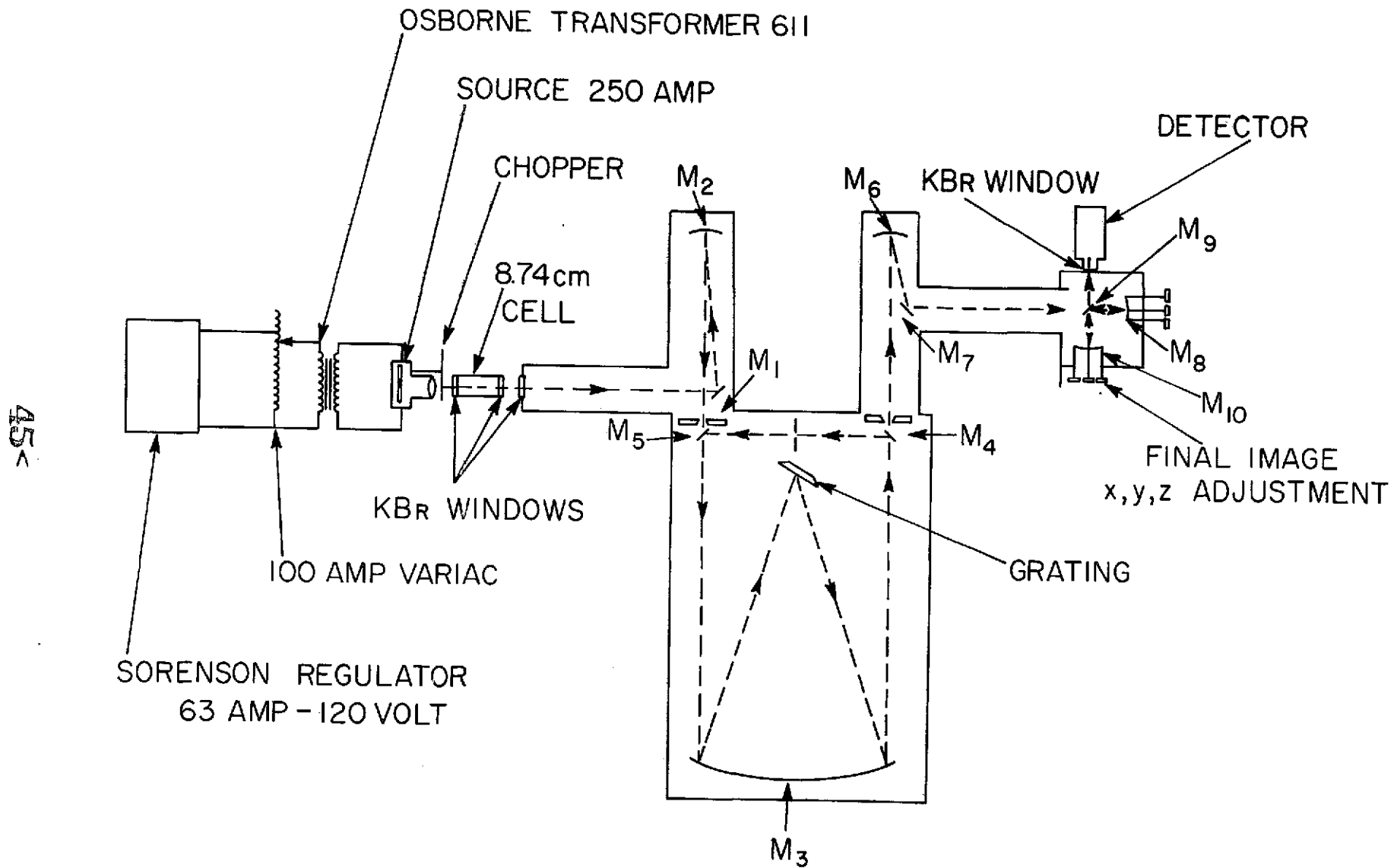


Fig. 3. Optical path diagram of complete instrument.

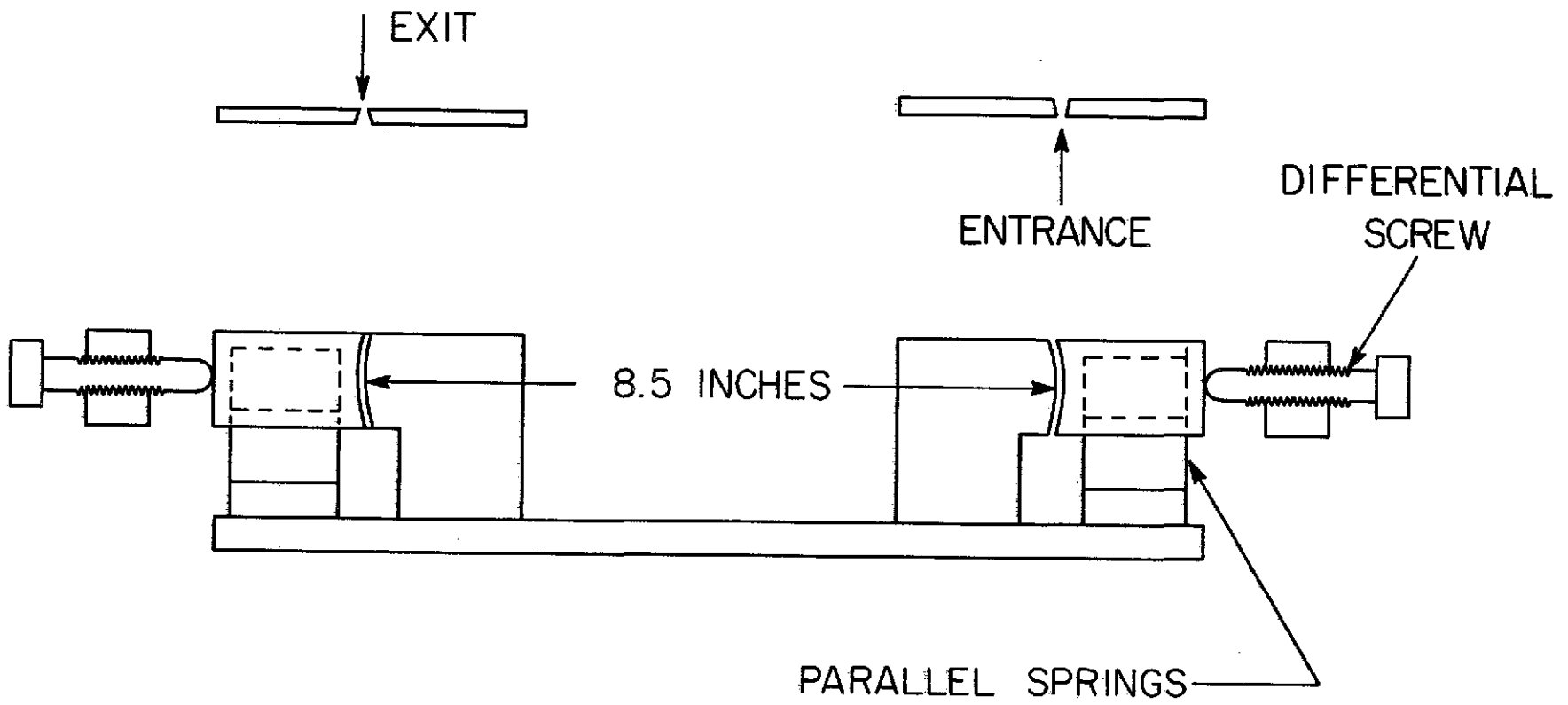


Fig. 4. Sketch of entrance and exit optics.

47<

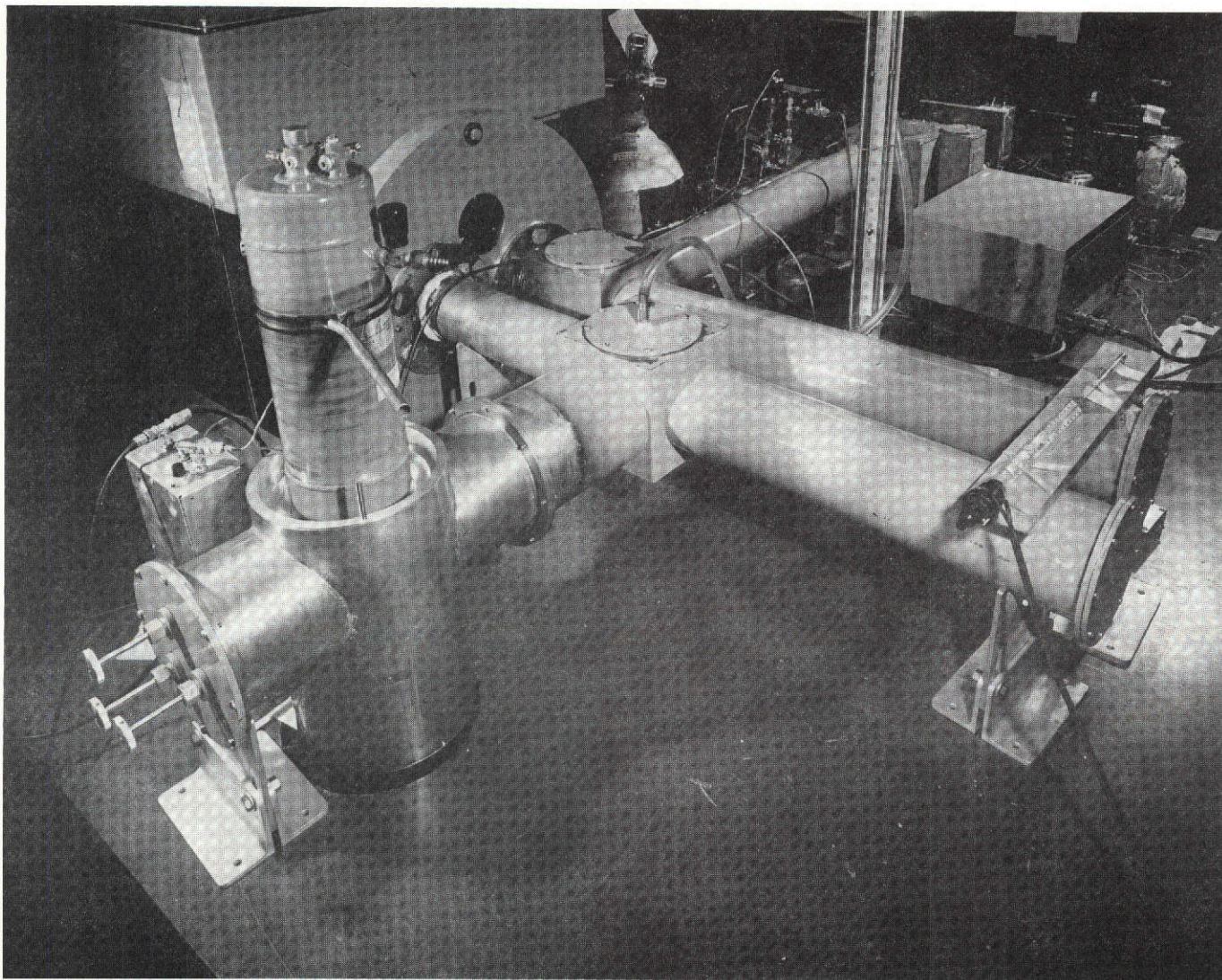


Fig. 5. Output Optics.



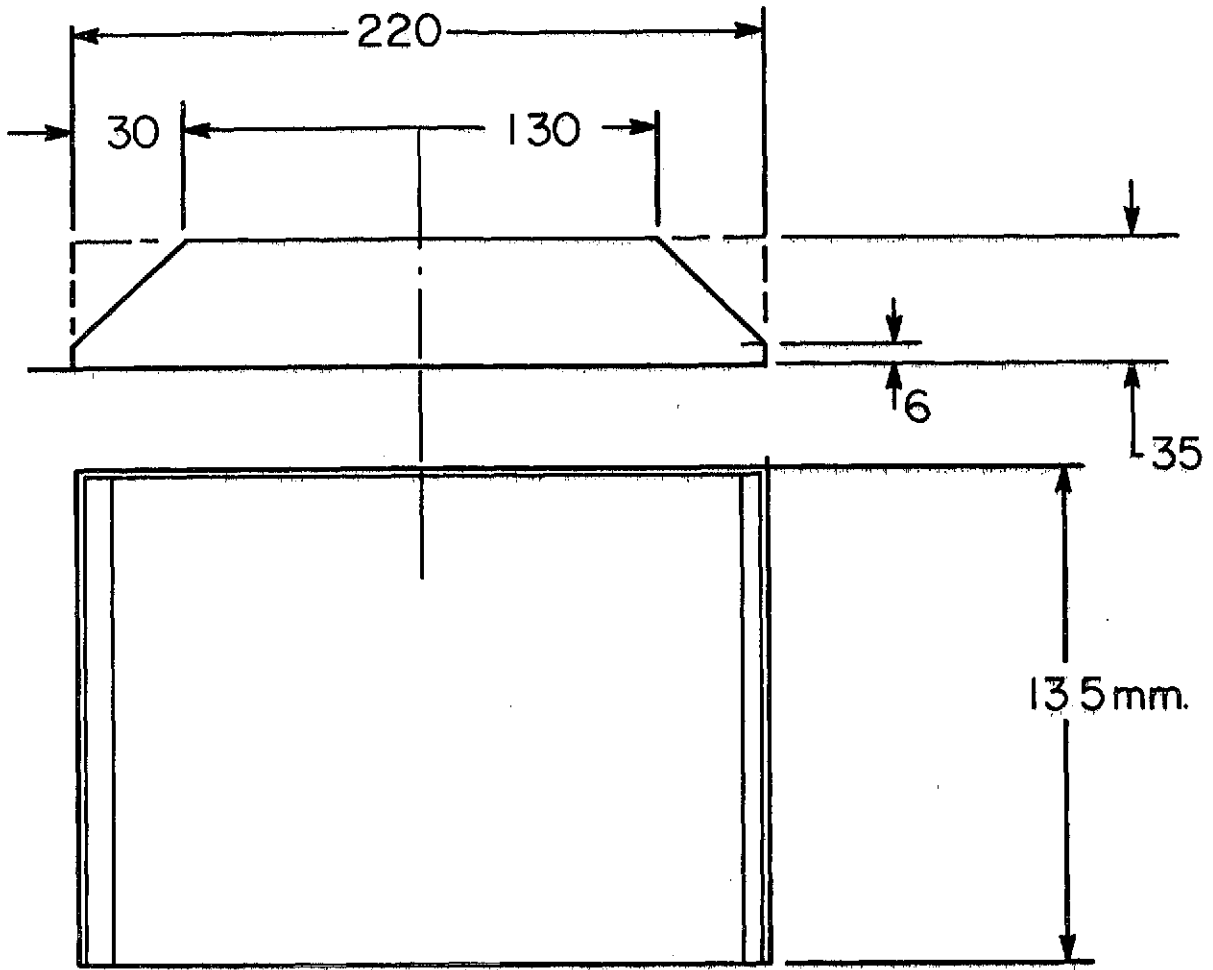


Fig. 6. Grating sketch, showing back corners removed.

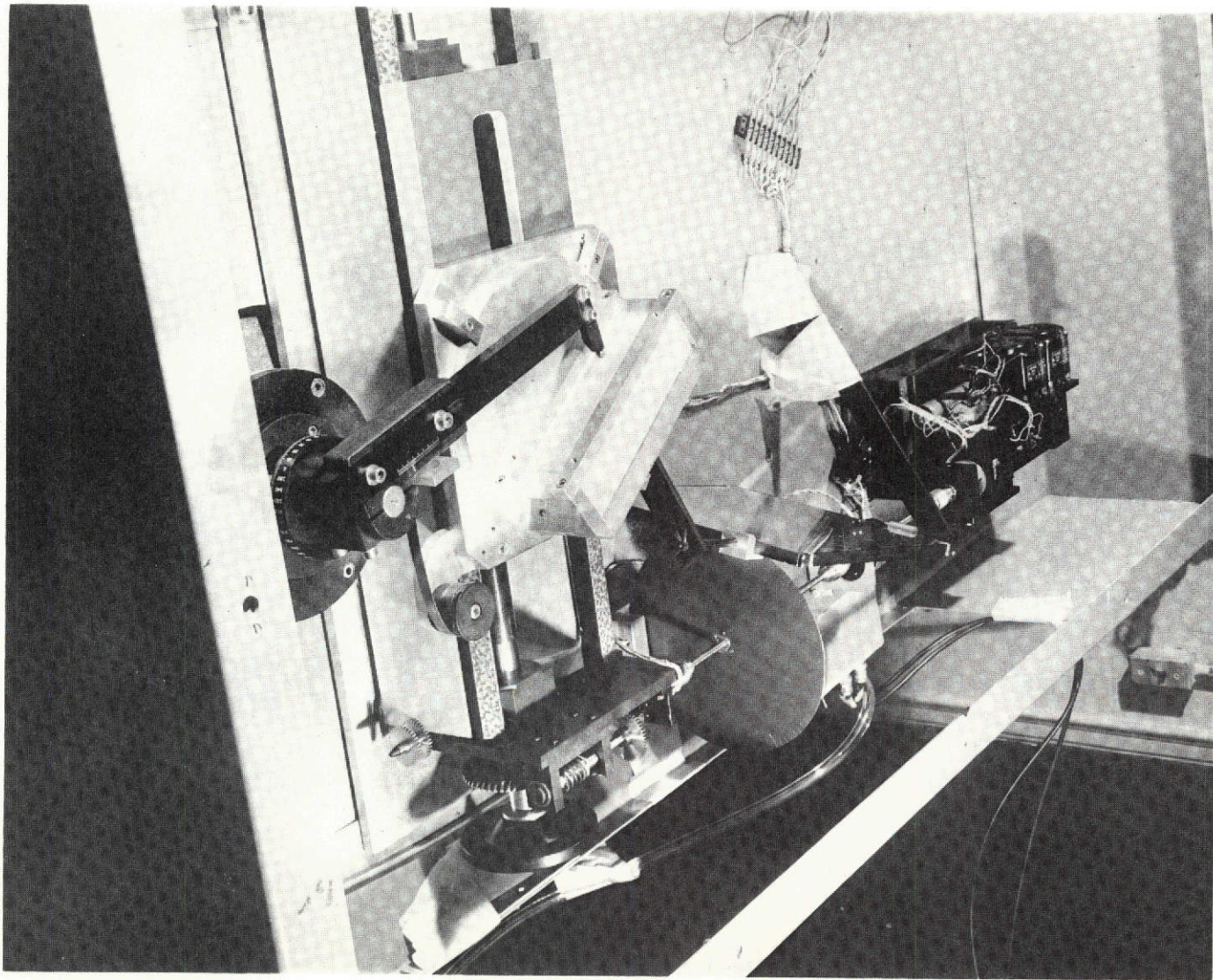
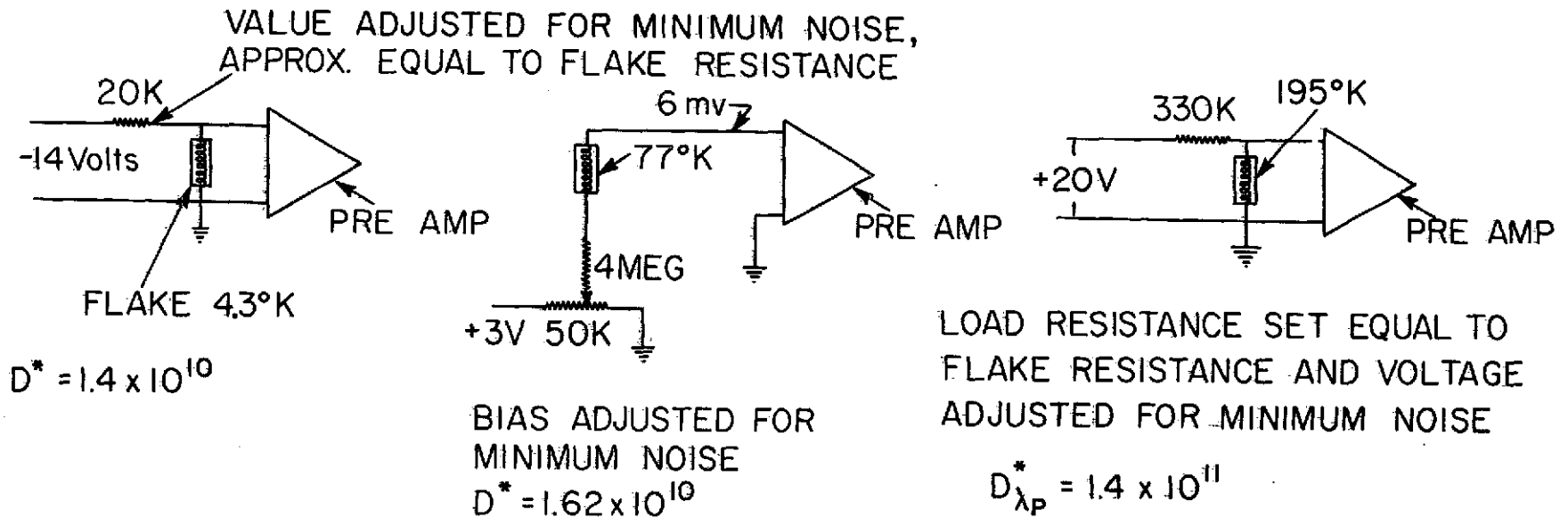


Fig. 7. Grating drive mechanism.

InSb TEXAS INSTRUMENT

CU: GE - TEXAS INSTRUMENT

PbS-O TYPE-EASTMAN



50  
A

Fig. 8. Detector bias circuits.

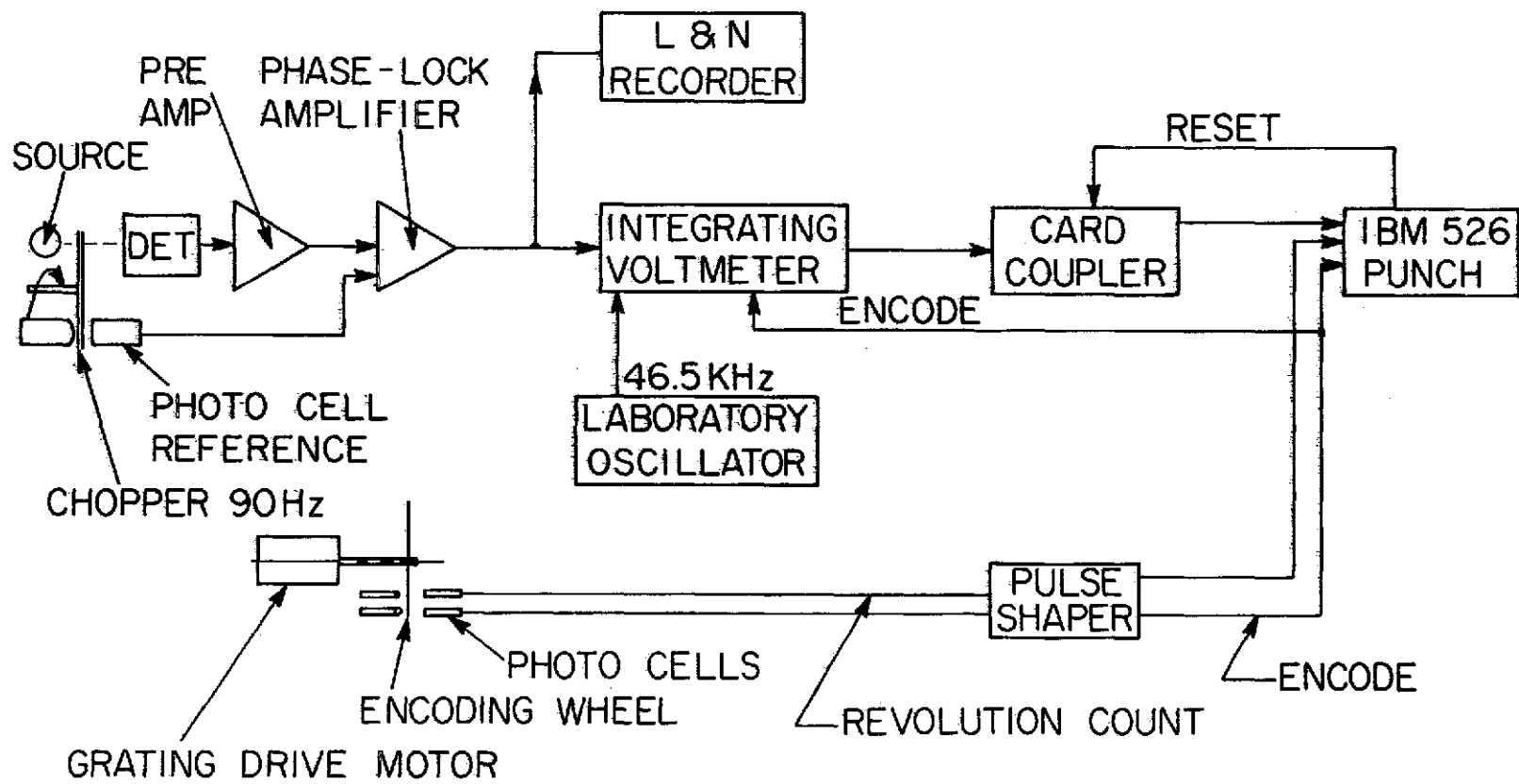


Fig. 9. Electrical block diagram of complete instrument.

57  
A

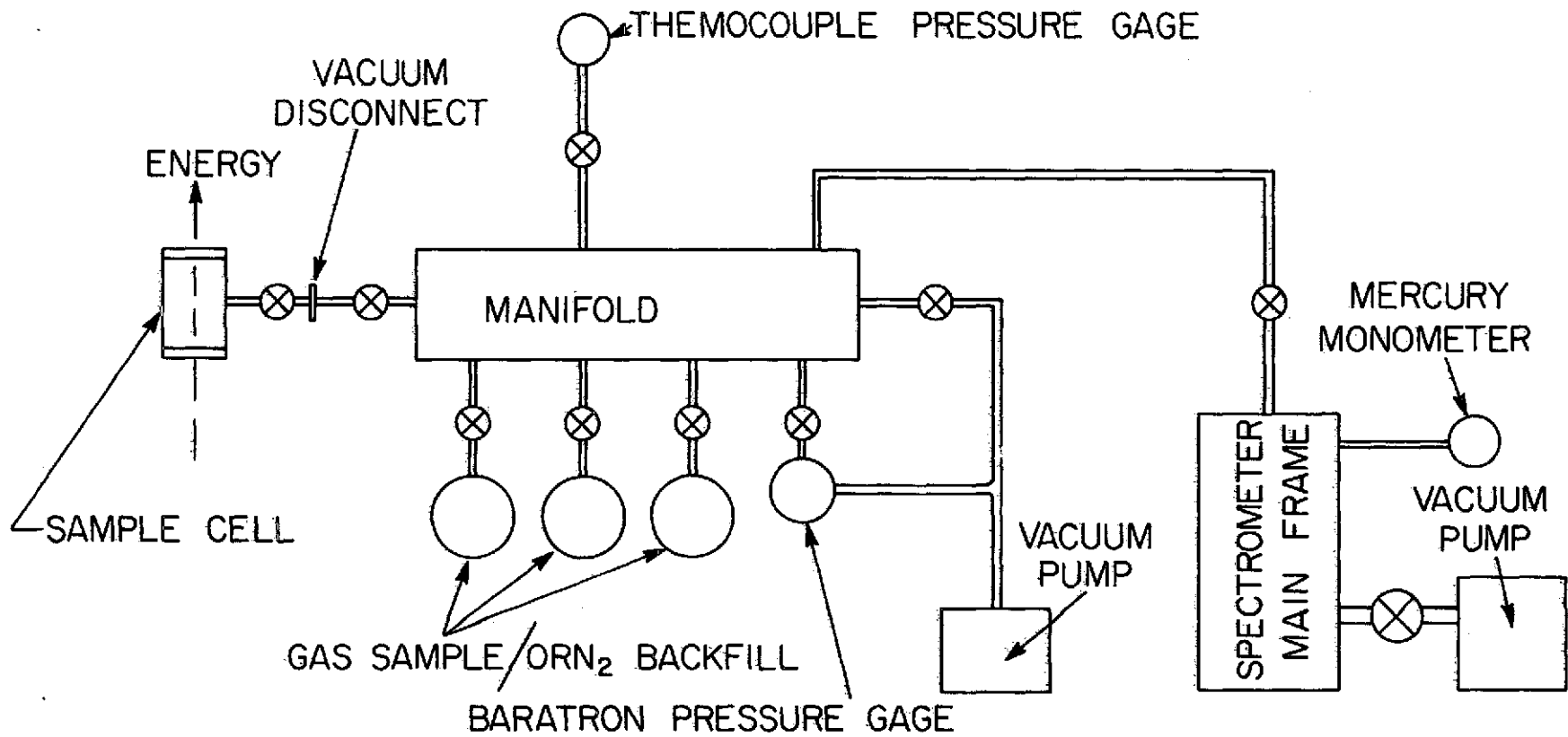


Fig. 10. Gas handling system schematic.

53 >

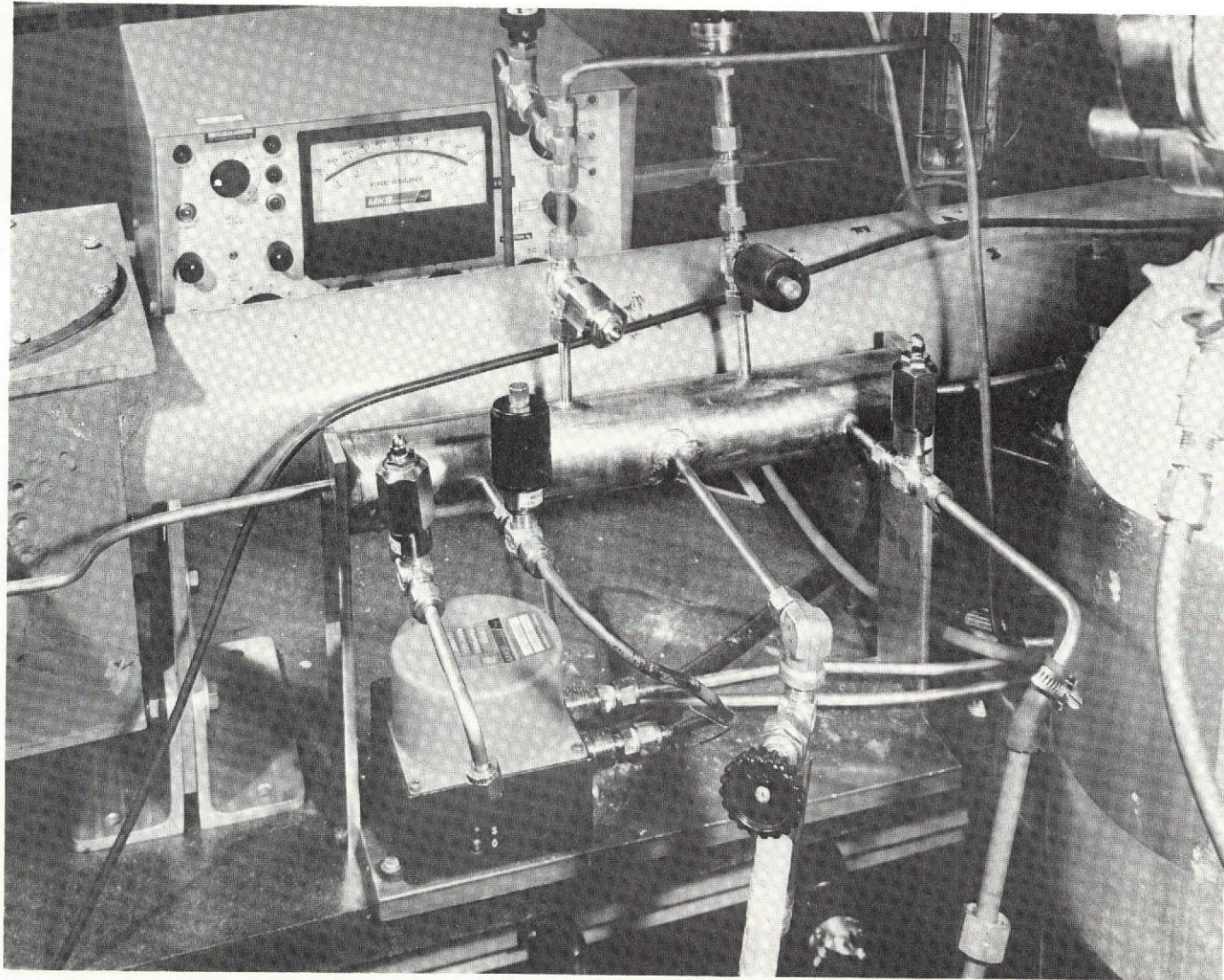


Fig. 11. Gas manifold.

SAC

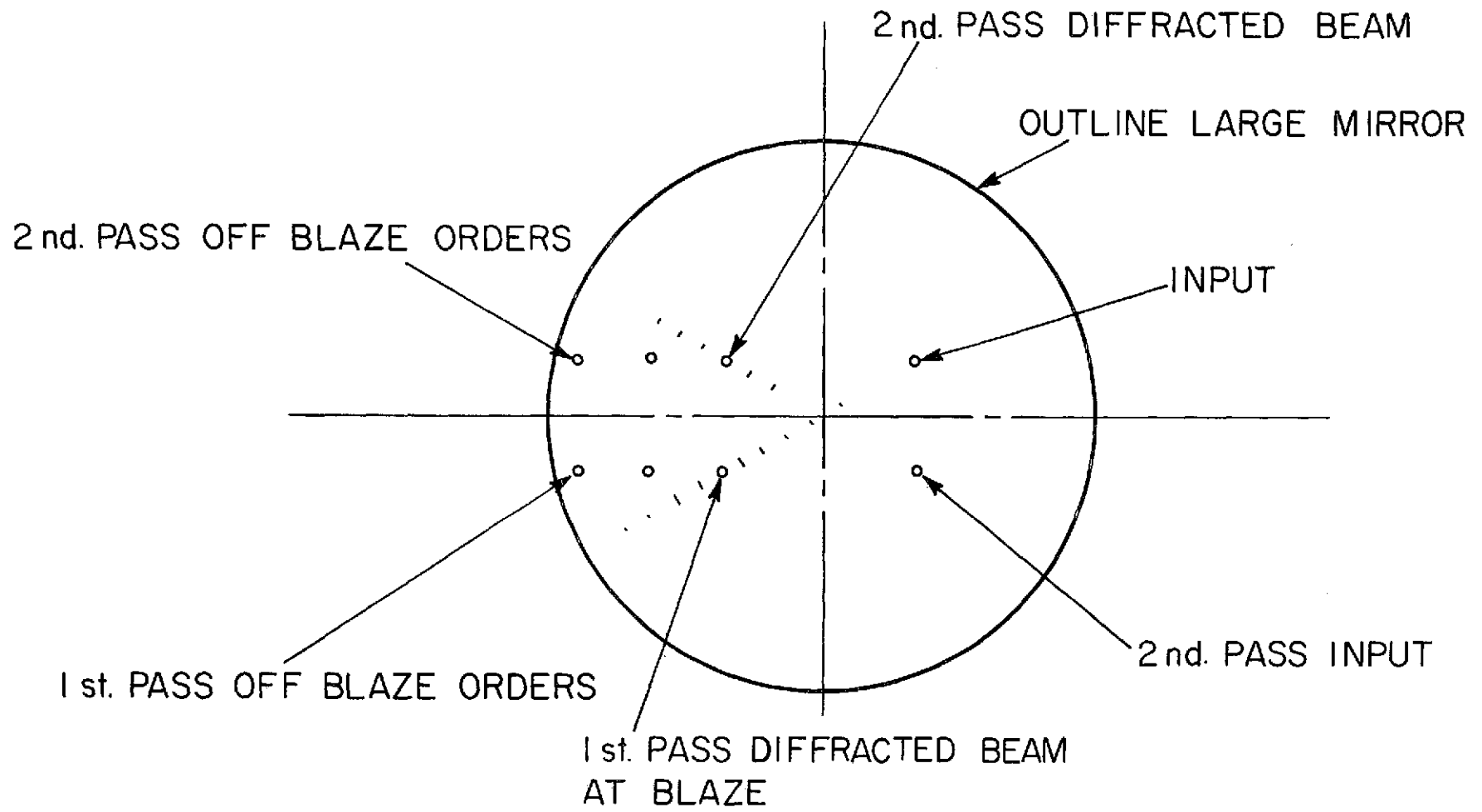


Fig. 12. Optical adjustment laser pattern.

FOLDOUT FRAME

FOLDOUT FRAME 2

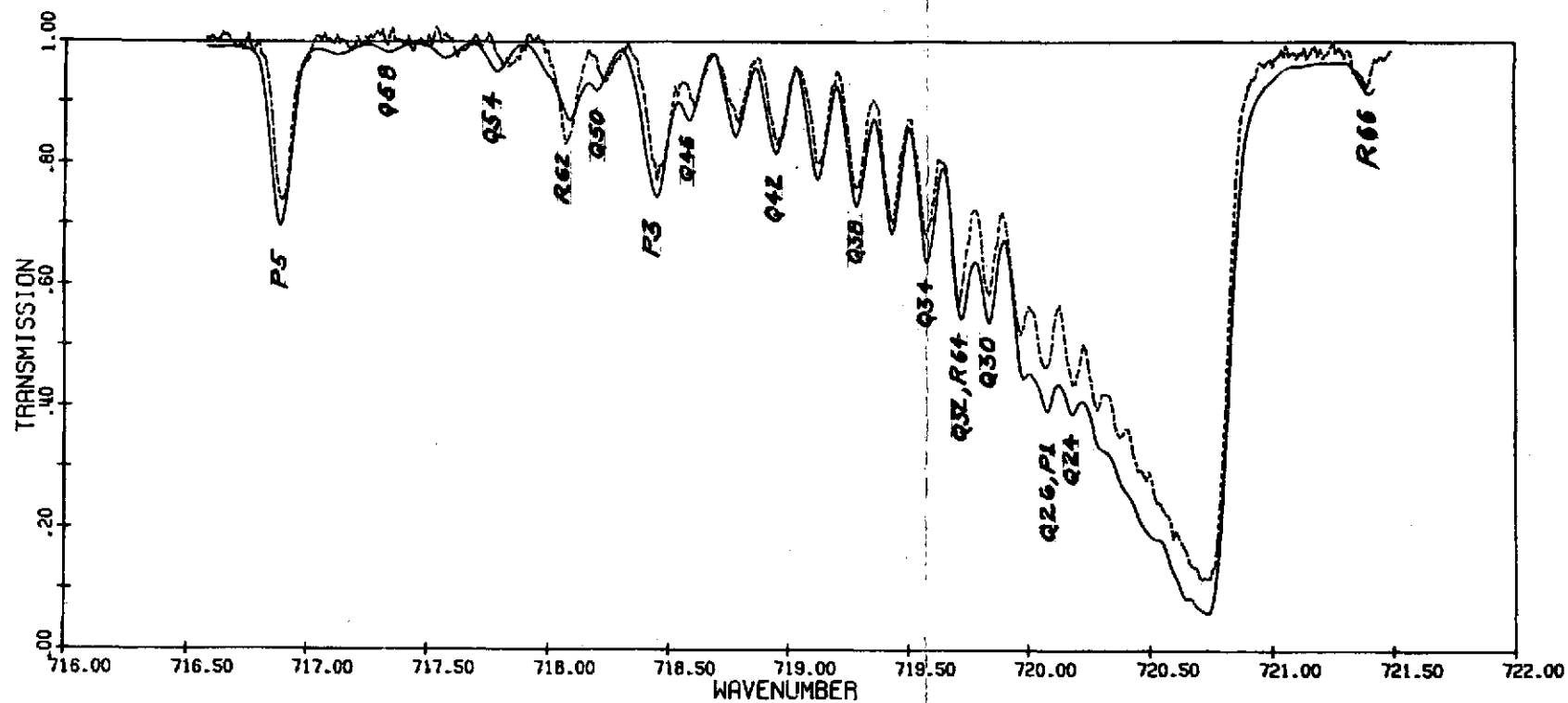


Fig. 13. Alternate resolution test. Comparison of theoretically computed spectrum (solid line) and measured spectrum (dotted line). The theoretical resolution is  $0.08 \text{ cm}^{-1}$ . Spectrum is of the P and Q branches of (010:1-100:0) band. Cell length = 8.74 cm, pressure 75.08 torr, temperature  $25^\circ\text{C}$ .

SCAN # 167

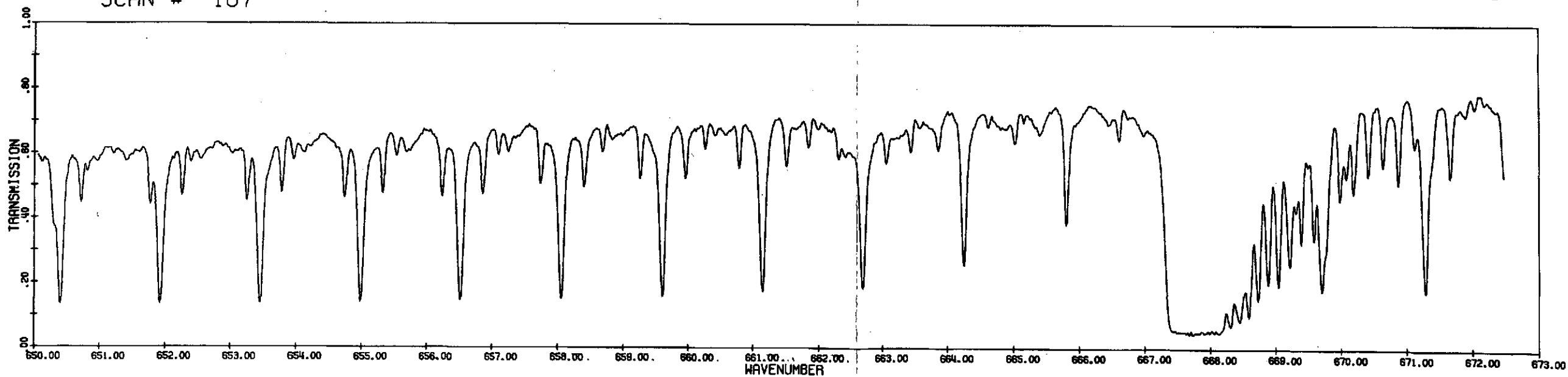


Fig. 14. Shows portions of the P, Q, and R branches of band (010:1-000:0) centered at  $667.38 \text{ cm}^{-1}$ . Cell length = 8.74 cm, pressure 30.0 torr, temperature  $24.5^\circ\text{C}$ .



SCAN # 168

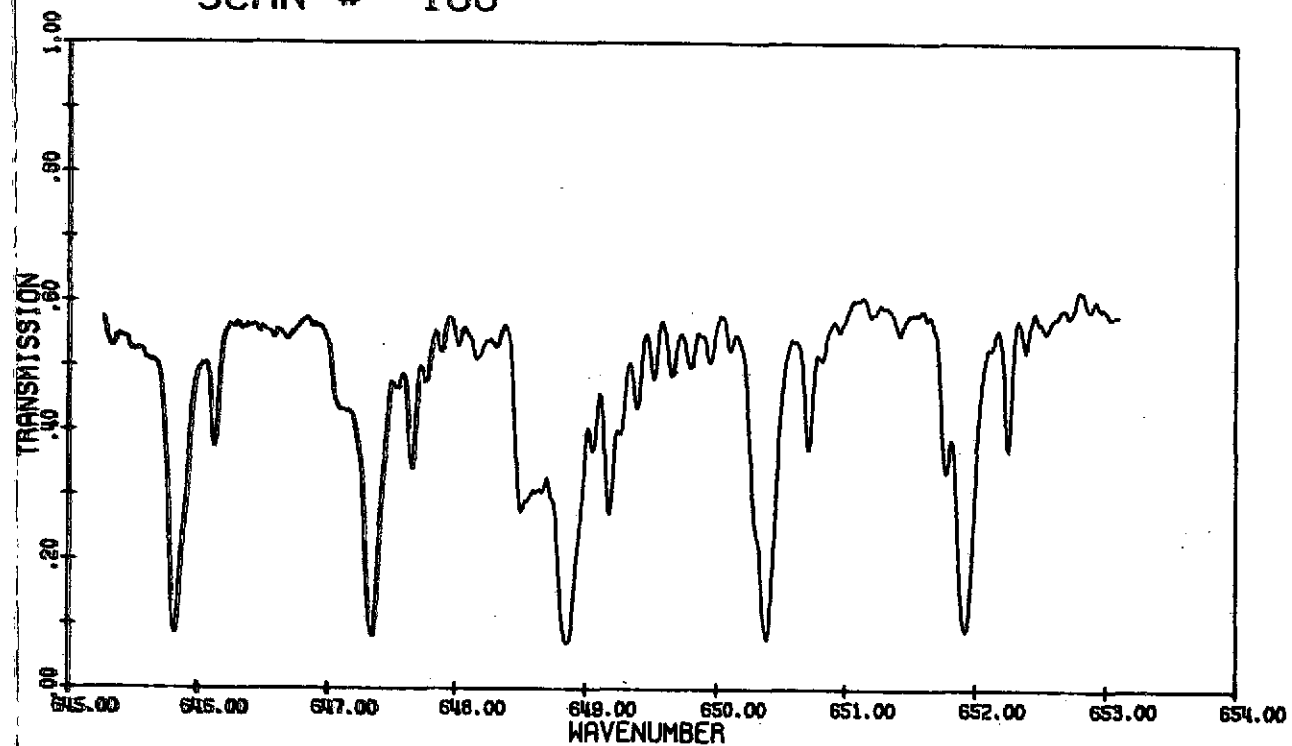


Fig. 15. Spectrum of Q branch of band [(110:1)II-(100:0)II] centered at  $647.06 \text{ cm}^{-1}$  and the  $^{13}\text{C}^{16}\text{O}_2$  isotopic Q branch of band (010:1-000:0). Cell length = 8.74 cm, pressure 50.0 torr, temperature  $24.5^\circ\text{C}$ .

SCAN # 173

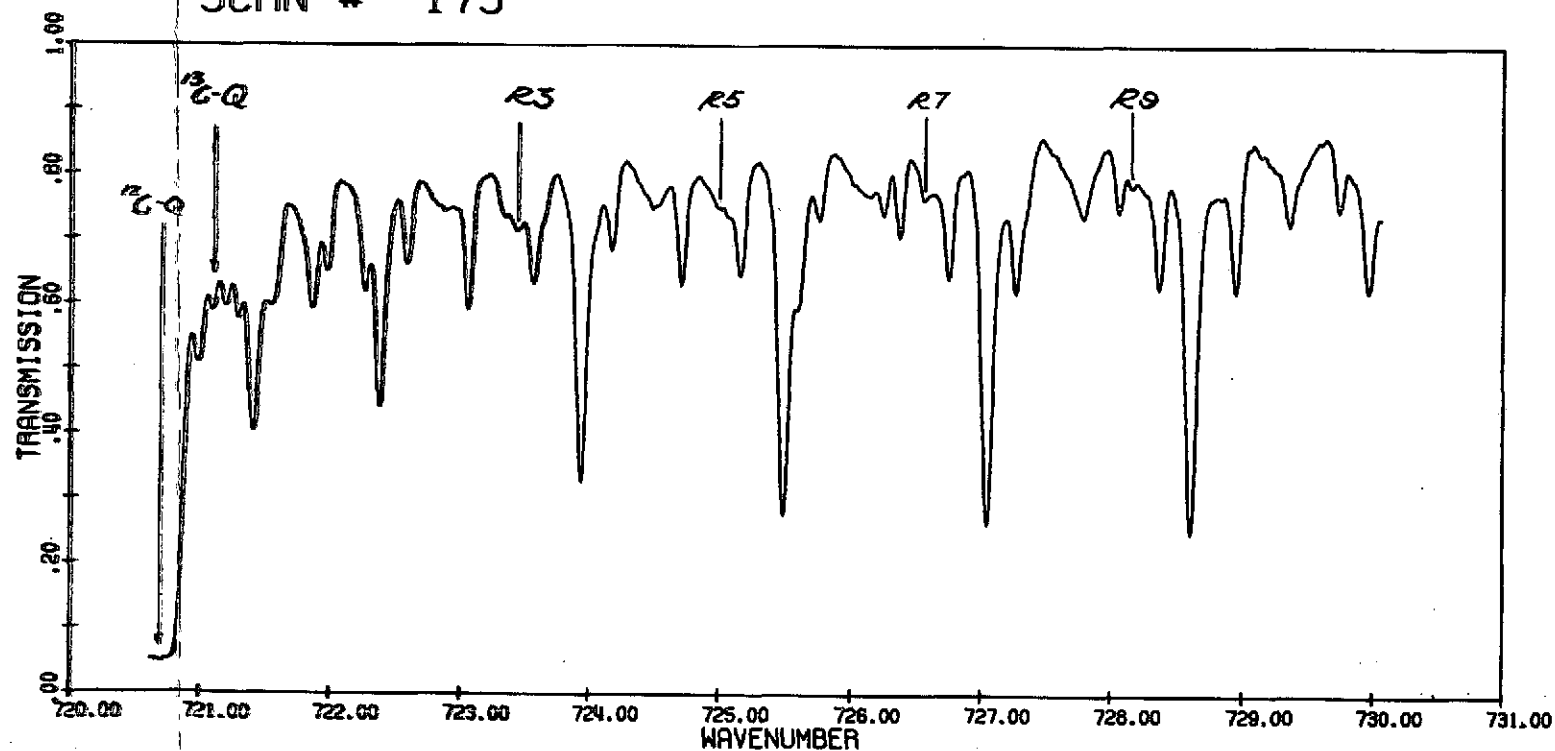


Fig. 16. The spectrum includes the Q branches of band [(100:0)I-010:1] centered at  $720.81 \text{ cm}^{-1}$ , the same band for the isotope  $^{13}\text{C}^{16}\text{O}_2$  centered at  $721.59 \text{ cm}^{-1}$ , and the identifiable R branch lines of the weak band [(200:0)I-(110:1)I] centered at  $720.29 \text{ cm}^{-1}$ . The ability to identify the R branch lines demonstrates the excellent signal to noise capability. Cell length = 20 meters, pressure 10.0 torr, temperature  $23.5^\circ\text{C}$ .

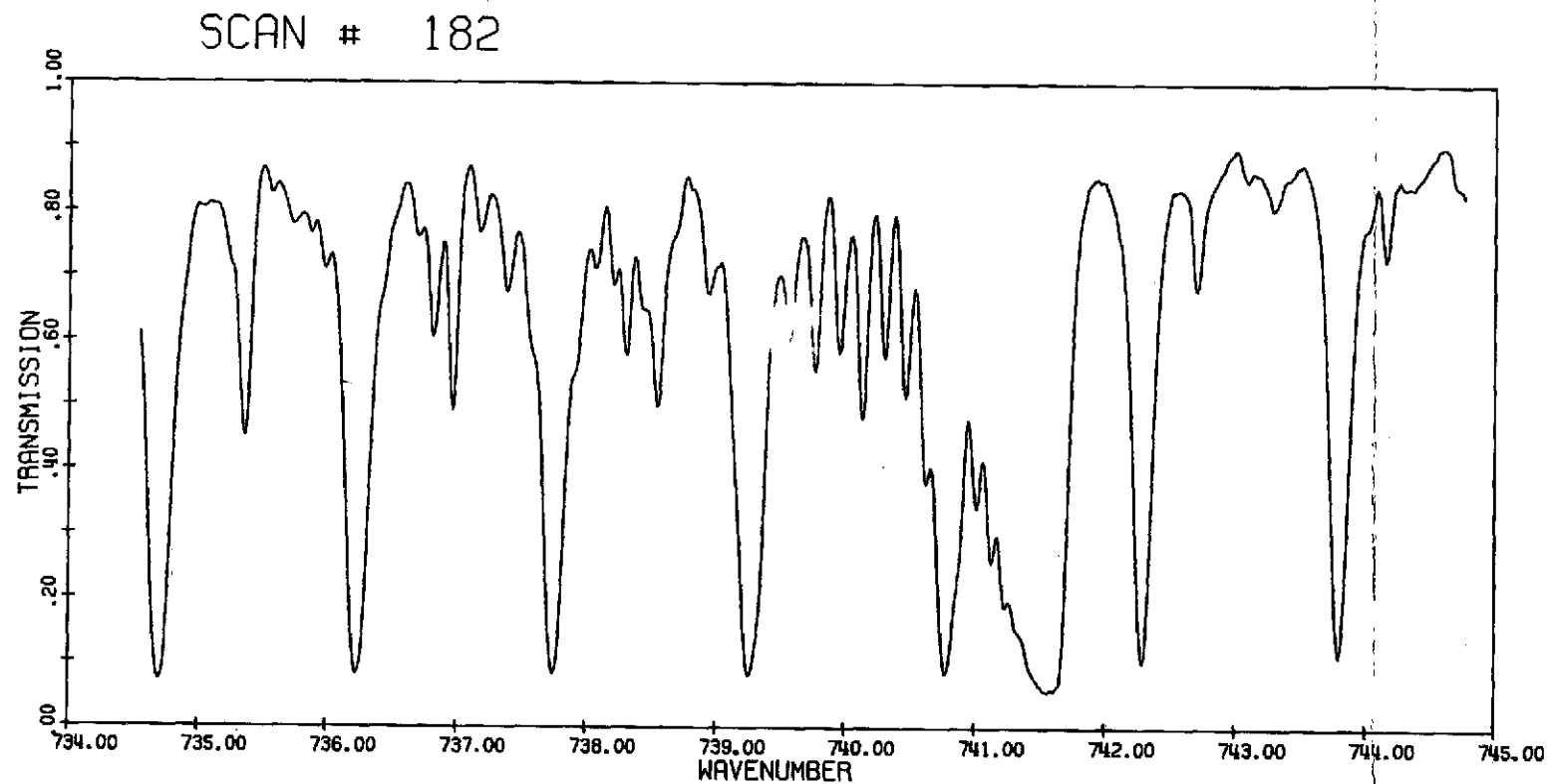


Fig. 17. Spectrum of the Q branch of band [ (110:1)I-020:2 ] centered at  $741.72 \text{ cm}^{-1}$  and the Q branch of band [ (200:0)II-(110:1)II ] centered at  $738.67 \text{ cm}^{-1}$ .  
Cell length = 20 meters, pressure 30.0 torr, temperature  $25.5^\circ\text{C}$ .

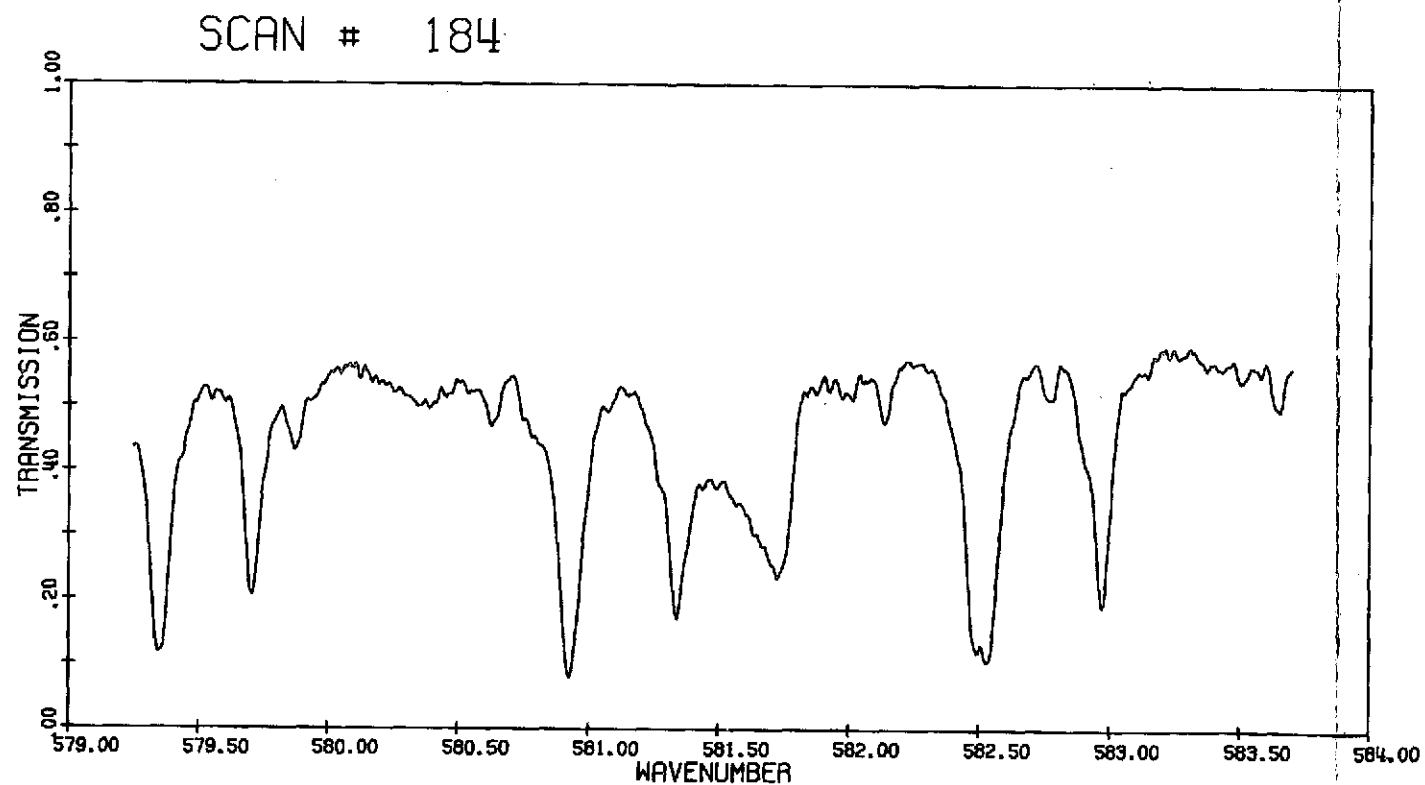


Fig. 18. Spectrum of Q branch of band [ (120:2)II-030:3 ] centered at  $581.7 \text{ cm}^{-1}$  in a region of poor signal to noise ratio.  
Cell length = 20 meters, pressure 50.0 torr, temperature  $26.5^\circ\text{C}$ .

SCAN # 198

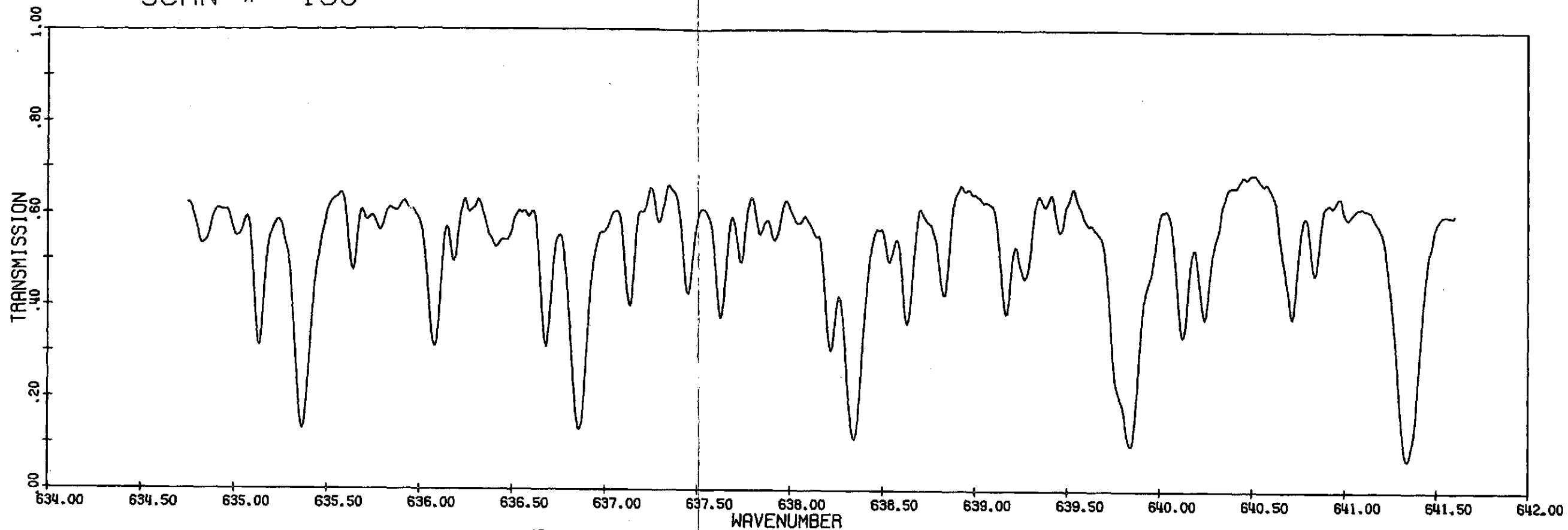


Fig. 19. Long path spectrum ( $634\text{ cm}^{-1}$ - $641\text{ cm}^{-1}$ ) which demonstrates the large number of lines which can be separated. Virtually every feature on the spectrum can be identified as a spectral line.

FOLDOUT FRAME

SCAN # 201

FOLDOUT FRAME

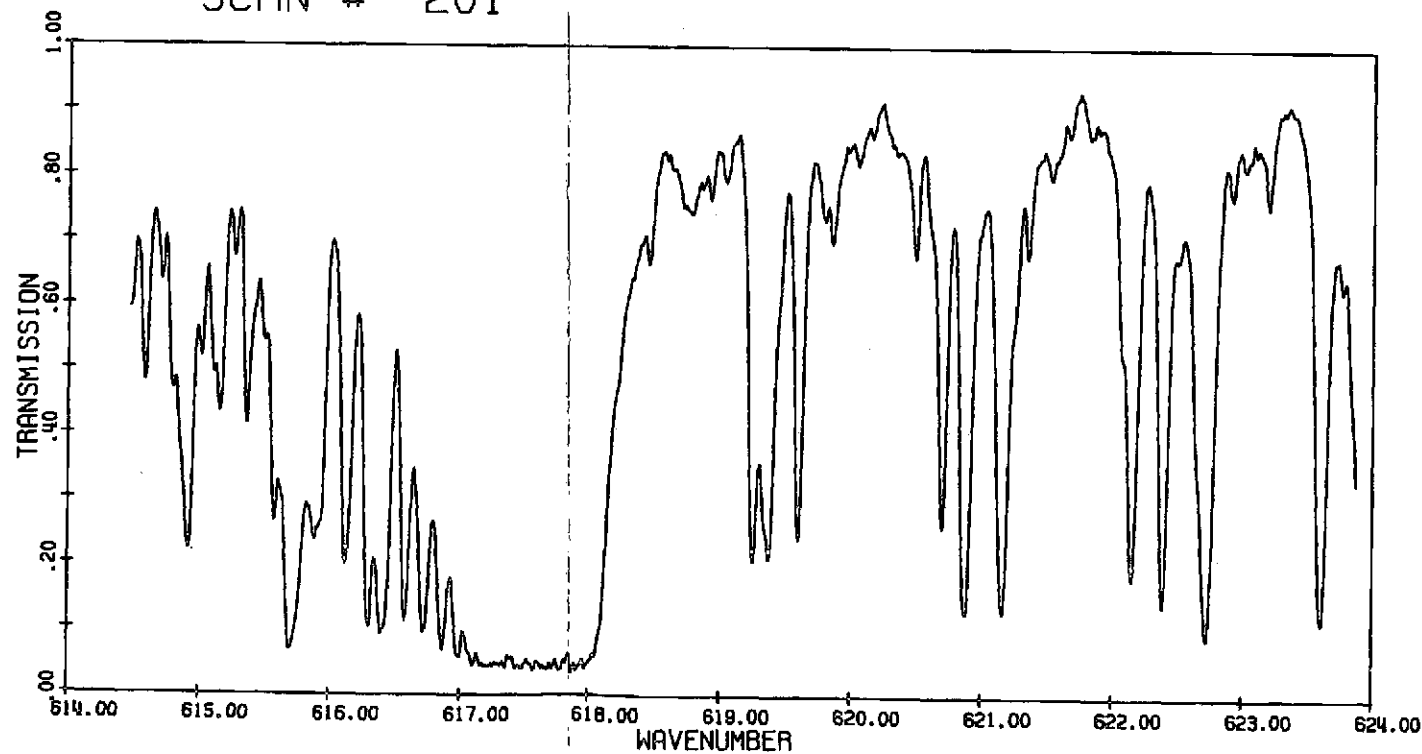
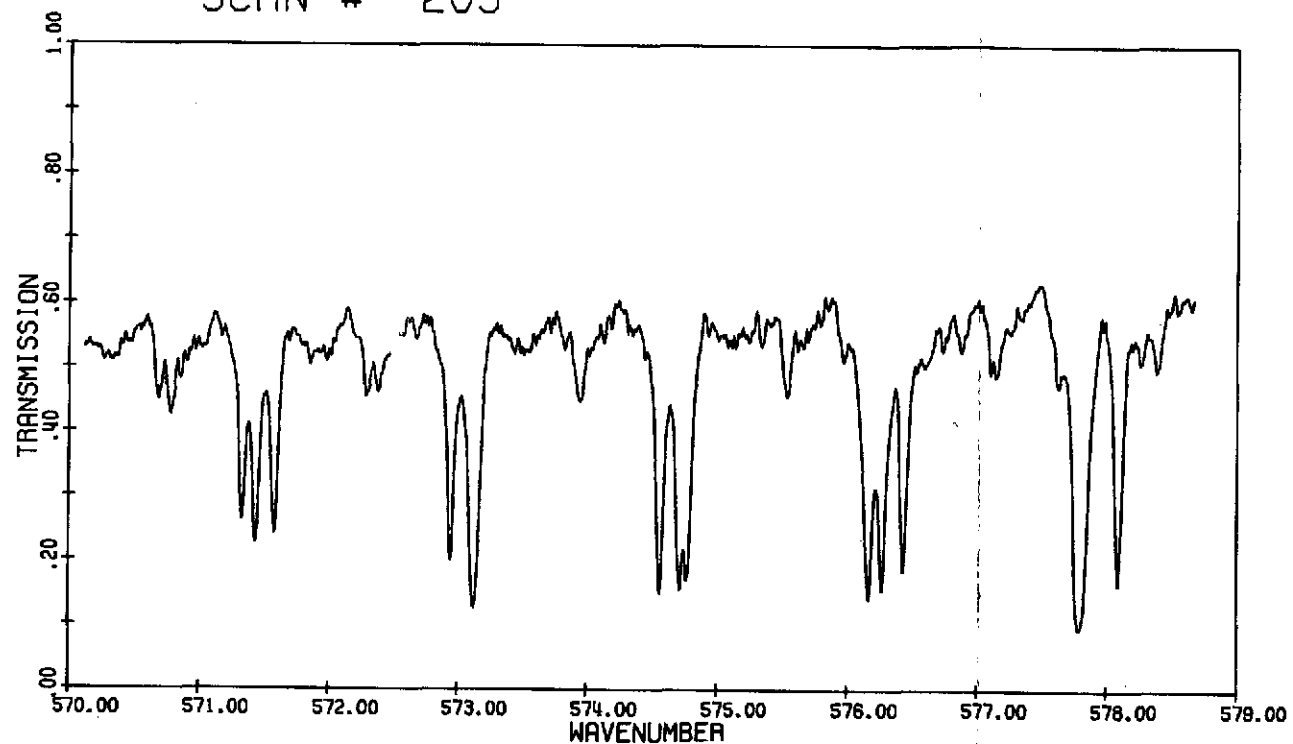


Fig. 20. Spectrum of the Q branch of band [ (100:0)II-010:1 ] centered at  $618.03\text{ cm}^{-1}$ . Cell length = 20 meters, pressure 26.0 torr, temperature  $22.5^{\circ}\text{C}$ .

SCAN # 203



FOLDOUT FRAME 1

FOLDOUT FRAME 2

Fig. 21. Example of how strong lines stand out in a noisy spectrum. The spectrum is dominated by the P branches of bands [ (100:0)II-010:1 ] and [ (110:1)II-020:2 ] Cell length = 20 meters, pressure 75.0 torr, temperature 22.5°C.

SCAN # 212

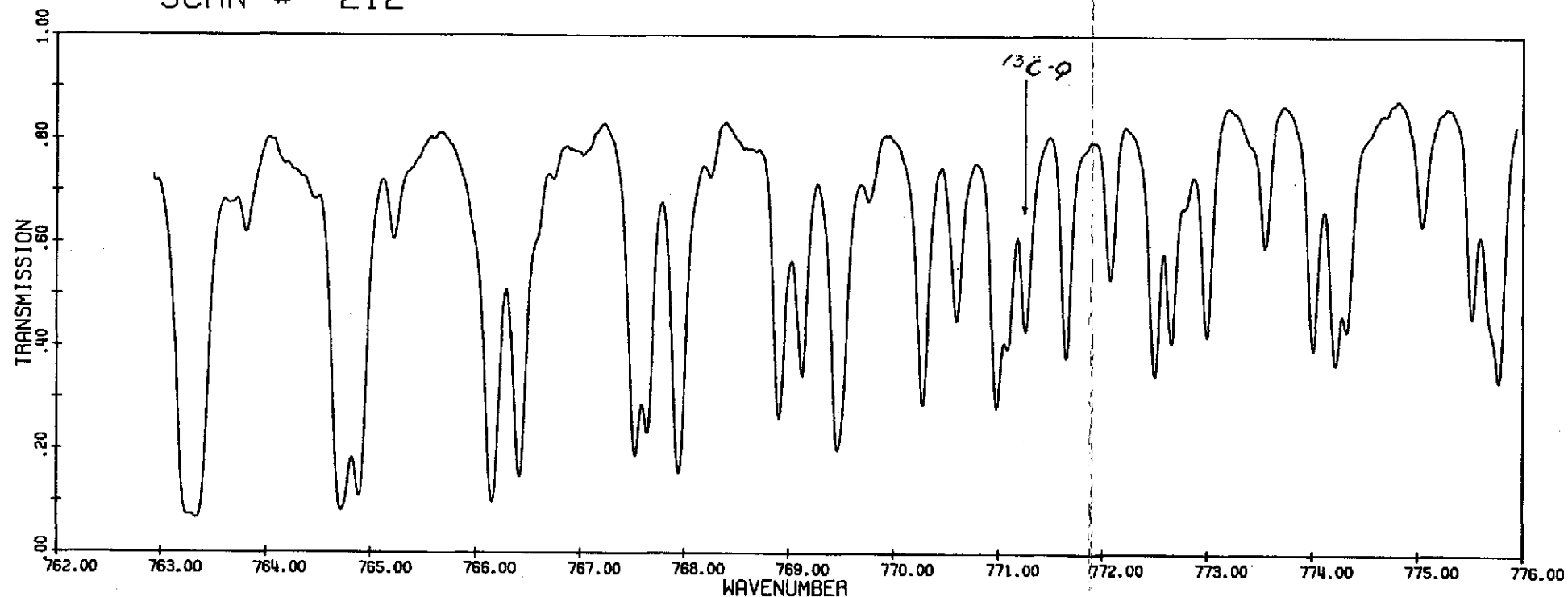


Fig. 22. Spectrum near  $770\text{ cm}^{-1}$ . The strongest absorption lines are the R branch of band [ (100:0)I-010:1 ] centered at  $720.81\text{ cm}^{-1}$  and band [ (110:1)I-020:2 ] centered at  $741.72\text{ cm}^{-1}$  and the P branch of band [ (110:1)I-(100:0)II ] centered at  $791.45\text{ cm}^{-1}$ . The anomalous feature at  $771.3\text{ cm}^{-1}$  is due to the unresolved lines of the Q branch of  $^{13}\text{C}^{16}\text{O}_2$  band [ (110:1)I-(100:0)II ]. Cell length = 20 meters., pressure 200 torr, temperature 23.2°C.

59

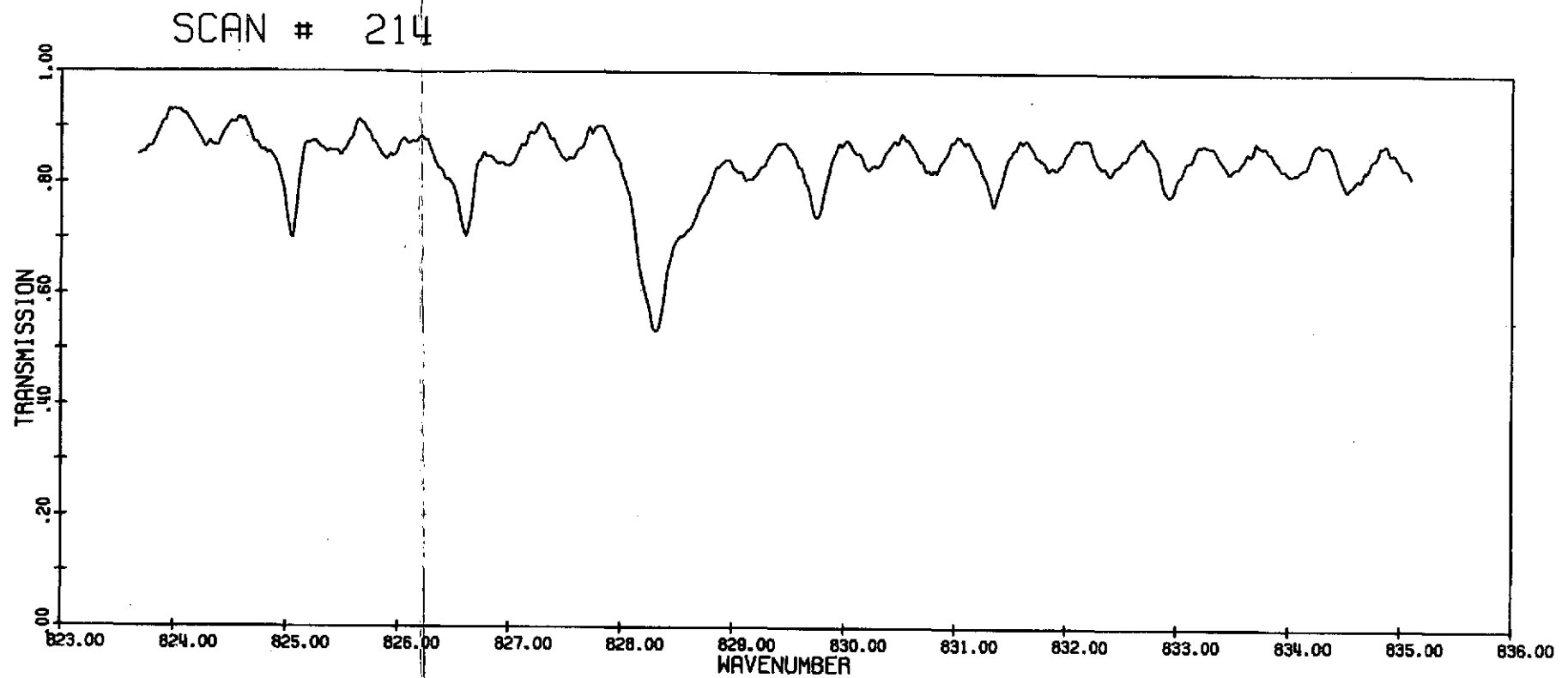


Fig. 23. The spectrum demonstrates the background variation problem due to the interference filter. The principal features are the Q branch of band [ (120:2)I-(110:1)II ] centered at  $823.23 \text{ cm}^{-1}$  and the R branch of [ (110:1)I-(100:0)II ] centered at  $791.45 \text{ cm}^{-1}$ . Cell length = 20 meters, pressure 420 torr, temperature  $23.4^\circ\text{C}$ .

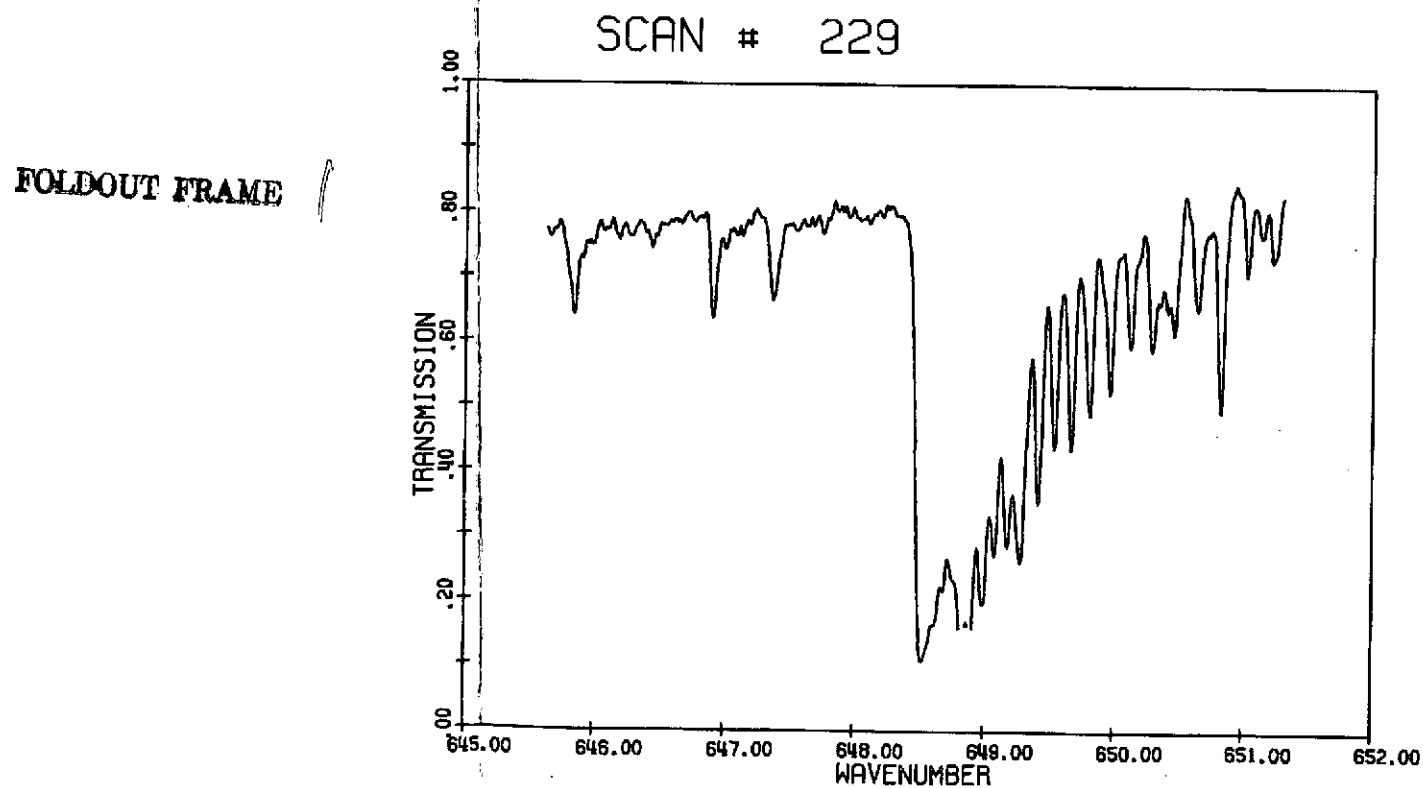


Fig. 24. Spectrum enriched in  $^{13}\text{C}^{16}\text{O}_2$  shows Q branch of (010:1-000:0) centered at  $648.48 \text{ cm}^{-1}$ . Cell length = 9.74 cm, pressure 30.0 torr, temperature  $24.8^\circ\text{C}$ .

SCAN # 236

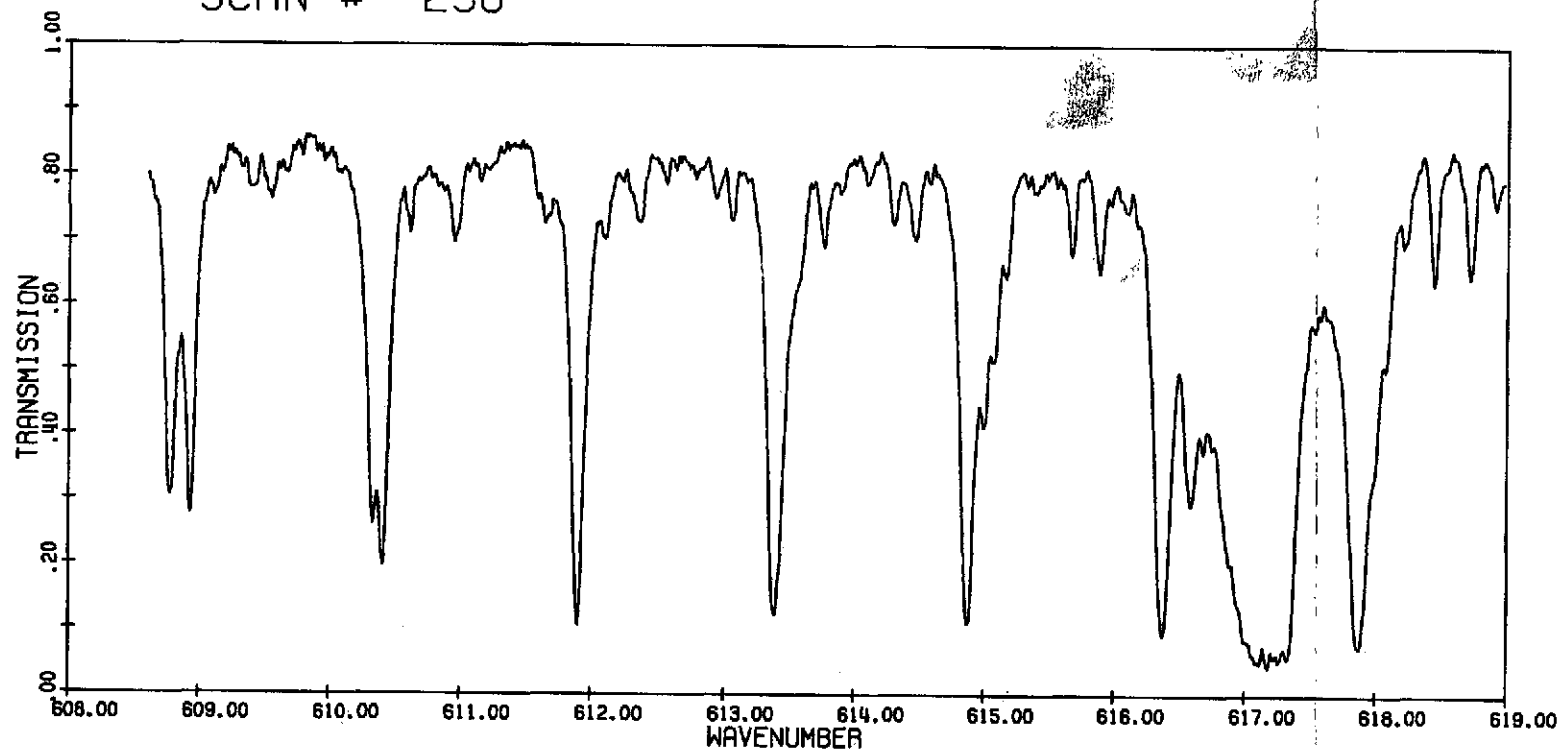


Fig. 25. Spectrum enriched in  $^{13}\text{C}^{16}\text{O}_2$  showing Q branch of band [(100:0)II-010:1]. Cell length = 8.74 cm, pressure 153 torr, temperature 23.5°C.

SCAN # 237

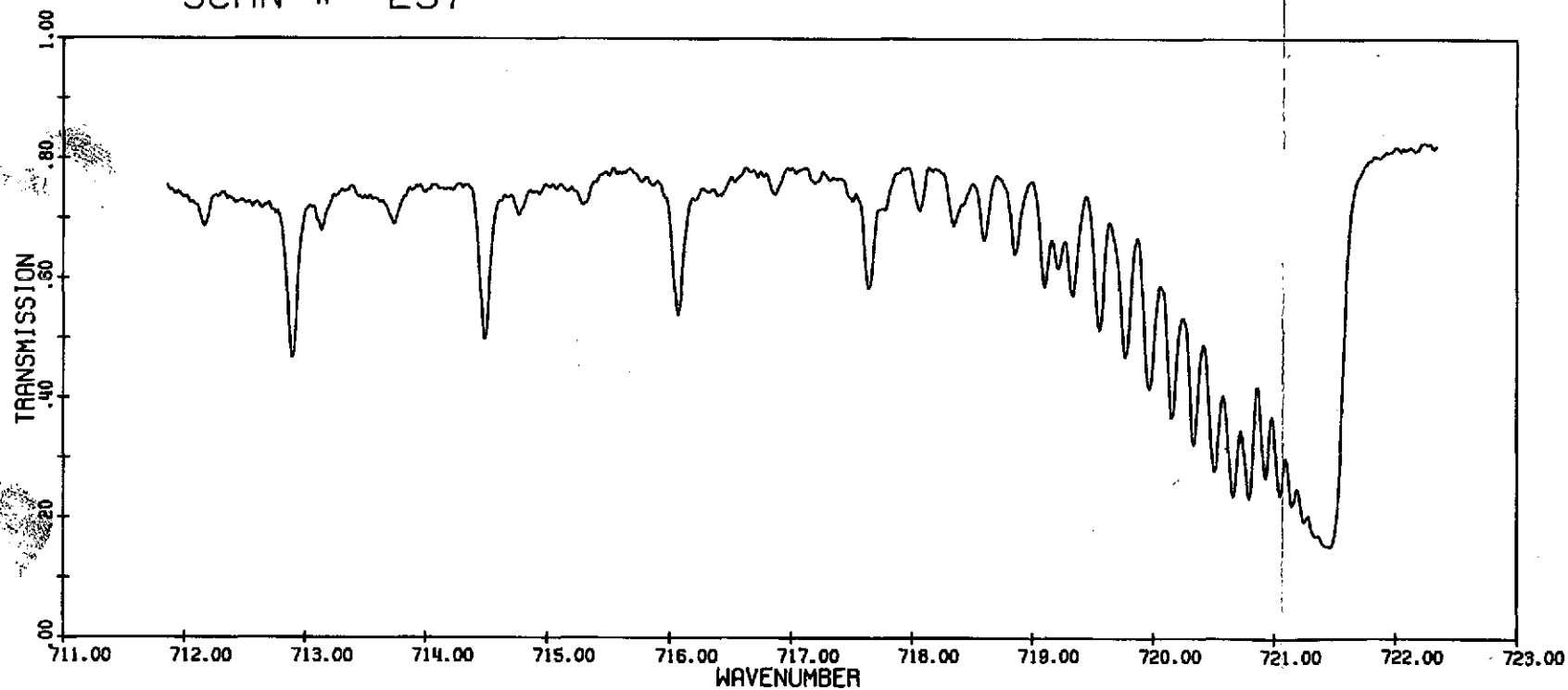
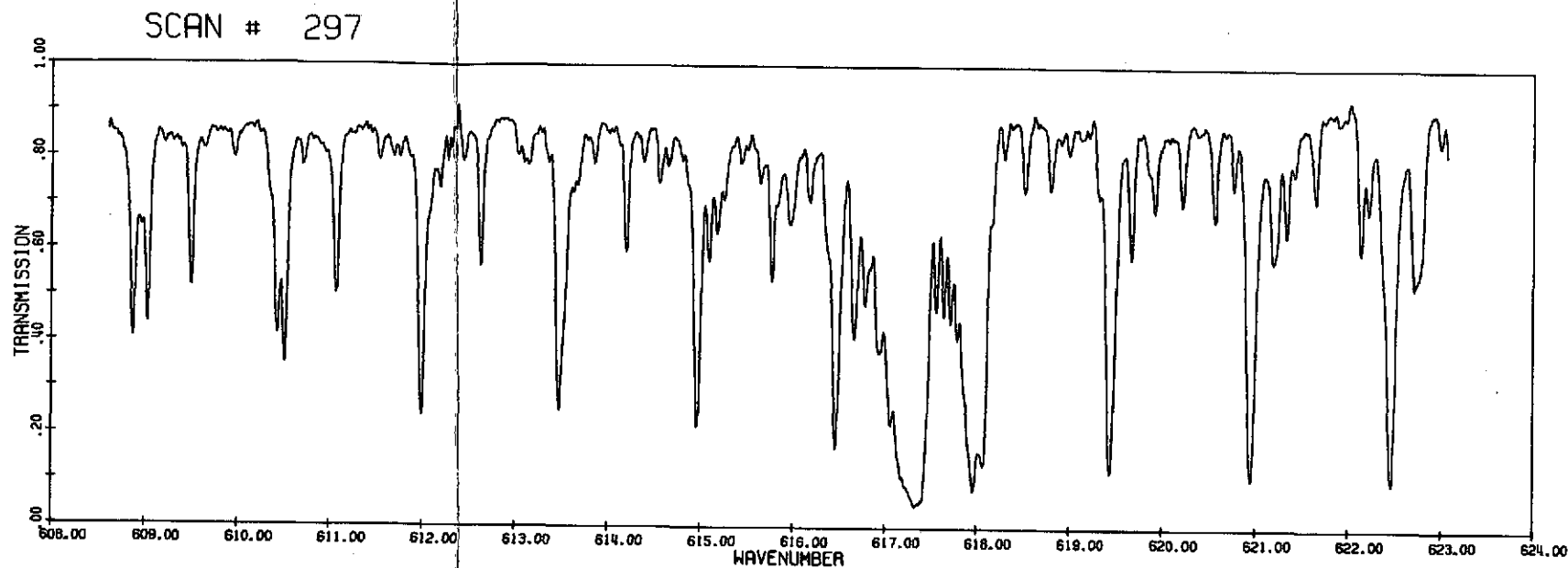


Fig. 26. Spectrum enriched in  $^{13}\text{C}^{16}\text{O}_2$  showing Q branch of band [(100:0)I-010:1]. Cell length = 8.74 cm, pressure 153 torr, temperature 23.5°C.

FOLDOUT FRAME 1



FOLDOUT FRAME 2

Fig. 27. Spectrum enriched in  $^{13}\text{C}^{16}\text{O}_2$  in 8.74 cm cell, pressure 75 torr, temperature  $24^\circ\text{C}$  and normal  $\text{CO}_2$  placed in 20 meter cell, pressure 2.4 torr. Resolution reduced to  $0.08\text{ cm}^{-1}$  to improve signal to noise ratio.

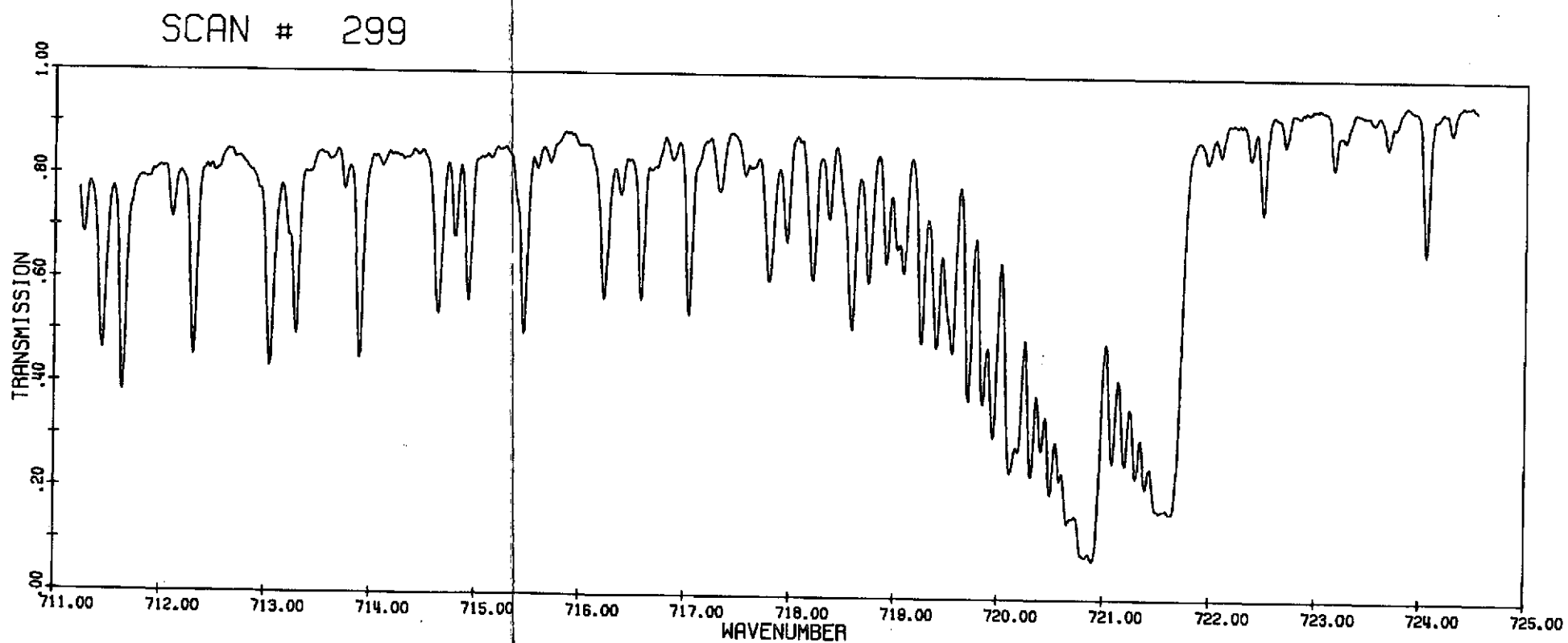


Fig. 28. Spectrum enriched in  $^{13}\text{C}^{16}\text{O}_2$  in 8.74 cm cell, pressure 150 torr, temperature  $24.2^\circ\text{C}$ . Normal  $\text{CO}_2$  in 20 meter cell, pressure 2.4 torr. The Q branches are band [ (100:0)I-(010:1) ]

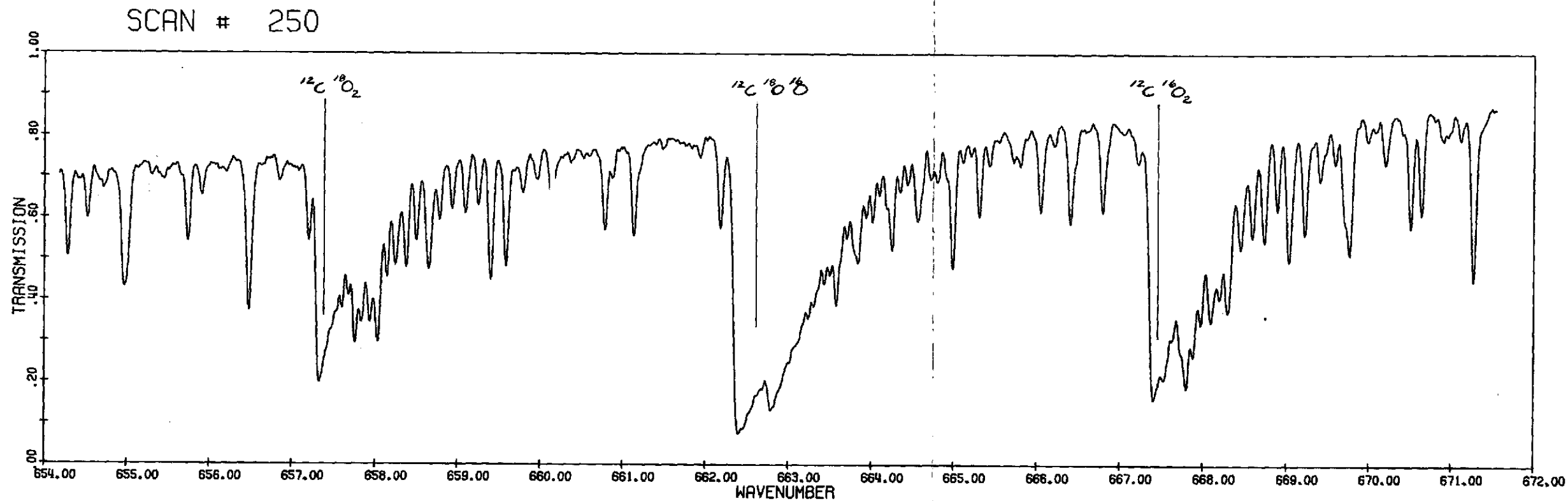


Fig. 29. Spectrum enriched in  $^{18}\text{O}$ . The prominent features are due to the  $\nu_2$  fundamental Q branches of the isotopic molecules  $^{12}\text{C}^{18}\text{O}_2$ ,  $^{12}\text{C}^{16}\text{O}^{18}\text{O}$ , and  $^{12}\text{C}^{16}\text{O}_2$ .  
Cell length = 8.74 cm, pressure 10.3 torr, temperature  $25^\circ\text{C}$ .

FOLDOUT FRAME

FOLDOUT FRAME 2

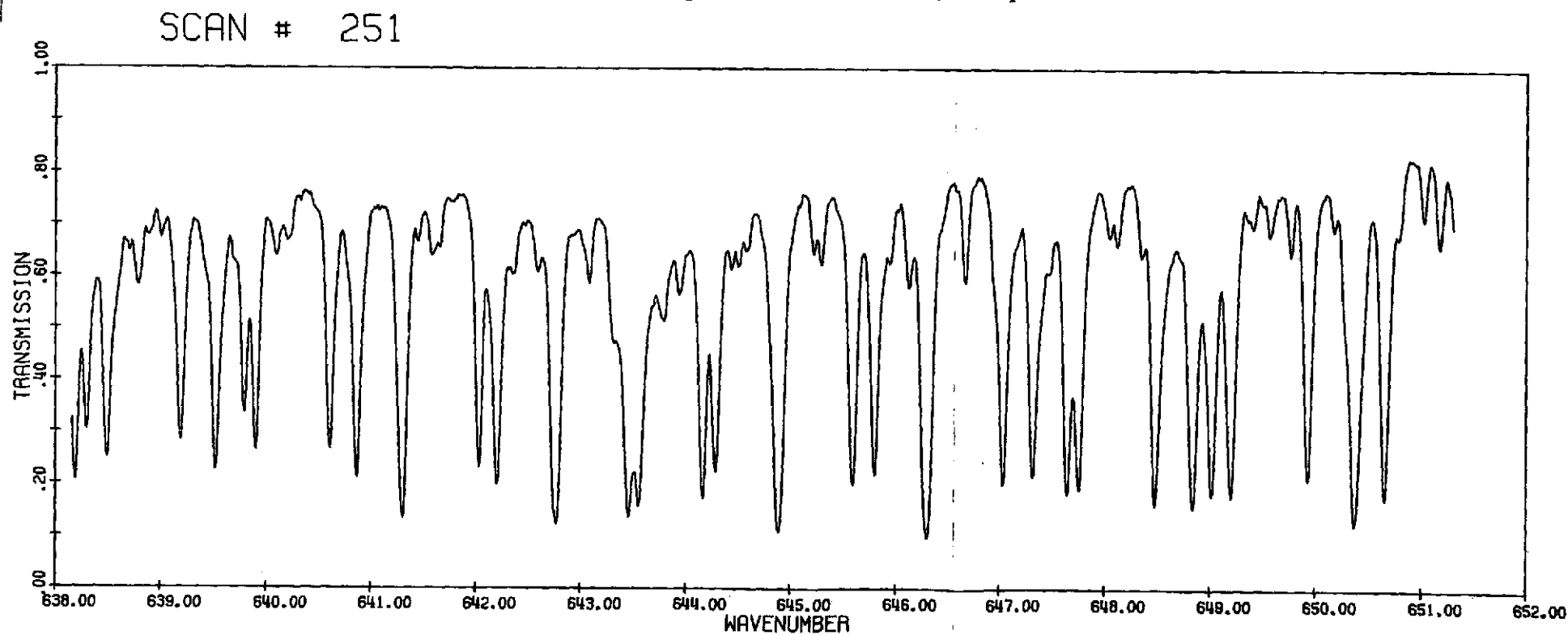
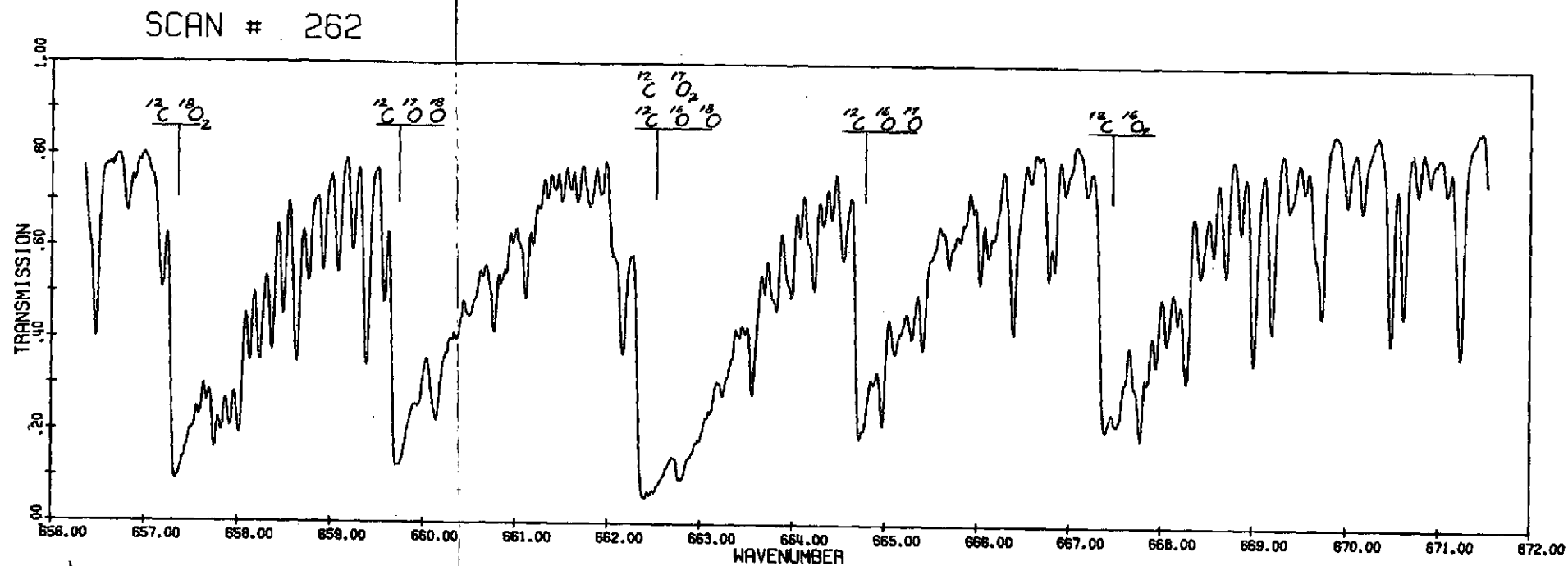


Fig. 30. Spectrum enriched in  $^{18}\text{O}$ . The strongest lines are due to the  $\nu_2$  fundamental and demonstrates the many lines which can be separated. Cell length 8.74 cm, pressure 49.8 torr, temperature  $25^\circ\text{C}$ .





FOLDOUT FRAME

Fig. 31. Spectrum enriched in  $^{17}\text{O}$  and  $^{18}\text{O}$ . The spectrum shows the Q branches of the  $\nu_2$  fundamental of the following isotopic molecules:  $^{12}\text{C}^{18}\text{O}_2$ ,  $^{12}\text{C}^{17}\text{O}^{18}\text{O}$ ,  $^{12}\text{C}^{16}\text{O}^{18}\text{O}$ ,  $^{12}\text{C}^{17}\text{O}_2$ ,  $^{12}\text{C}^{16}\text{O}^{17}\text{O}$ , and  $^{12}\text{C}^{16}\text{O}_2$ .  
Cell length = 8.74 cm, pressure 15 torr, temperature  $25^\circ\text{C}$ .

FOLDOUT FRAME

2

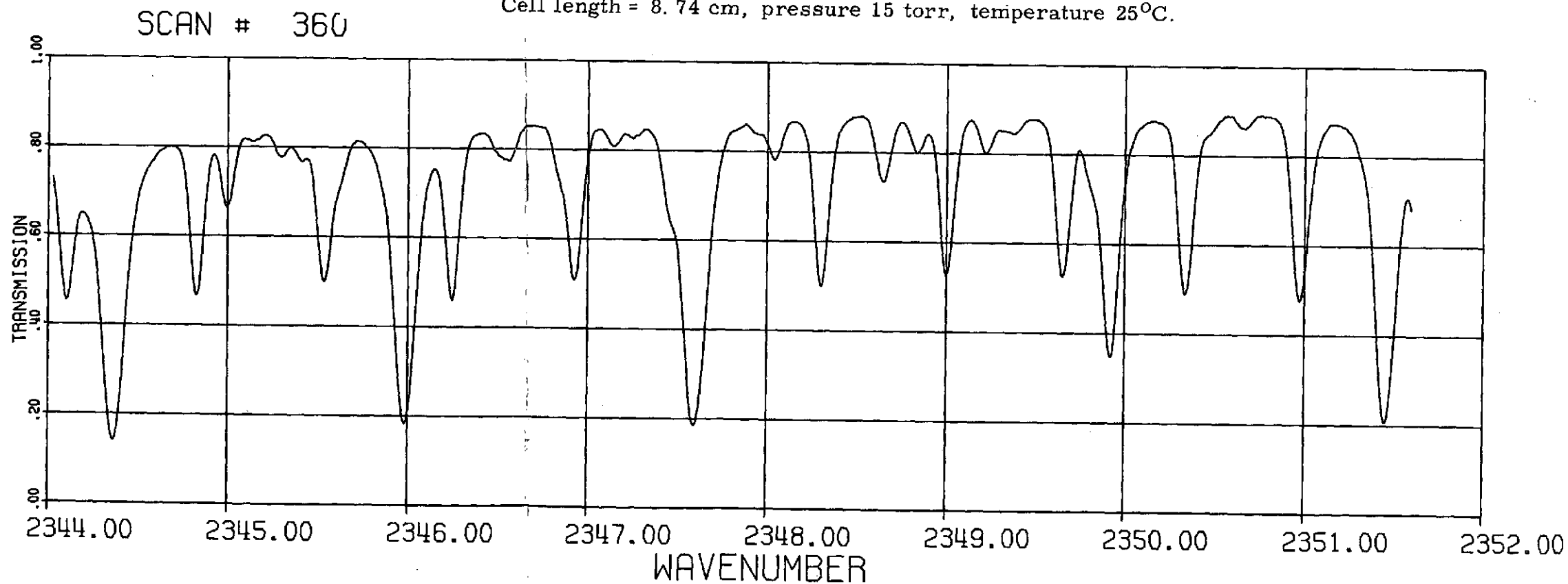


Fig. 32. Spectrum near the band center of the  $\nu_3$  fundamental of  $\text{CO}_2$ . An example of the spectrum obtained during the self-broadening study. Cell length = 8.74 cm, pressure 10.0 torr, temperature  $28^\circ\text{C}$ .

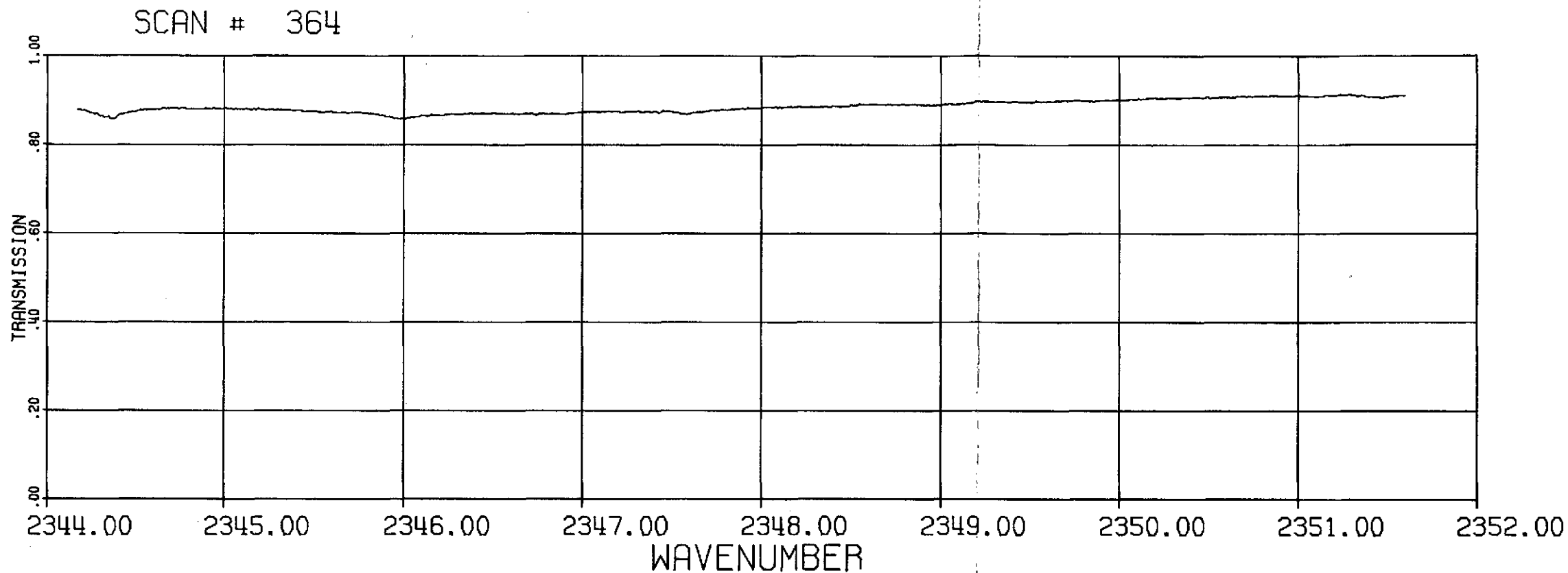
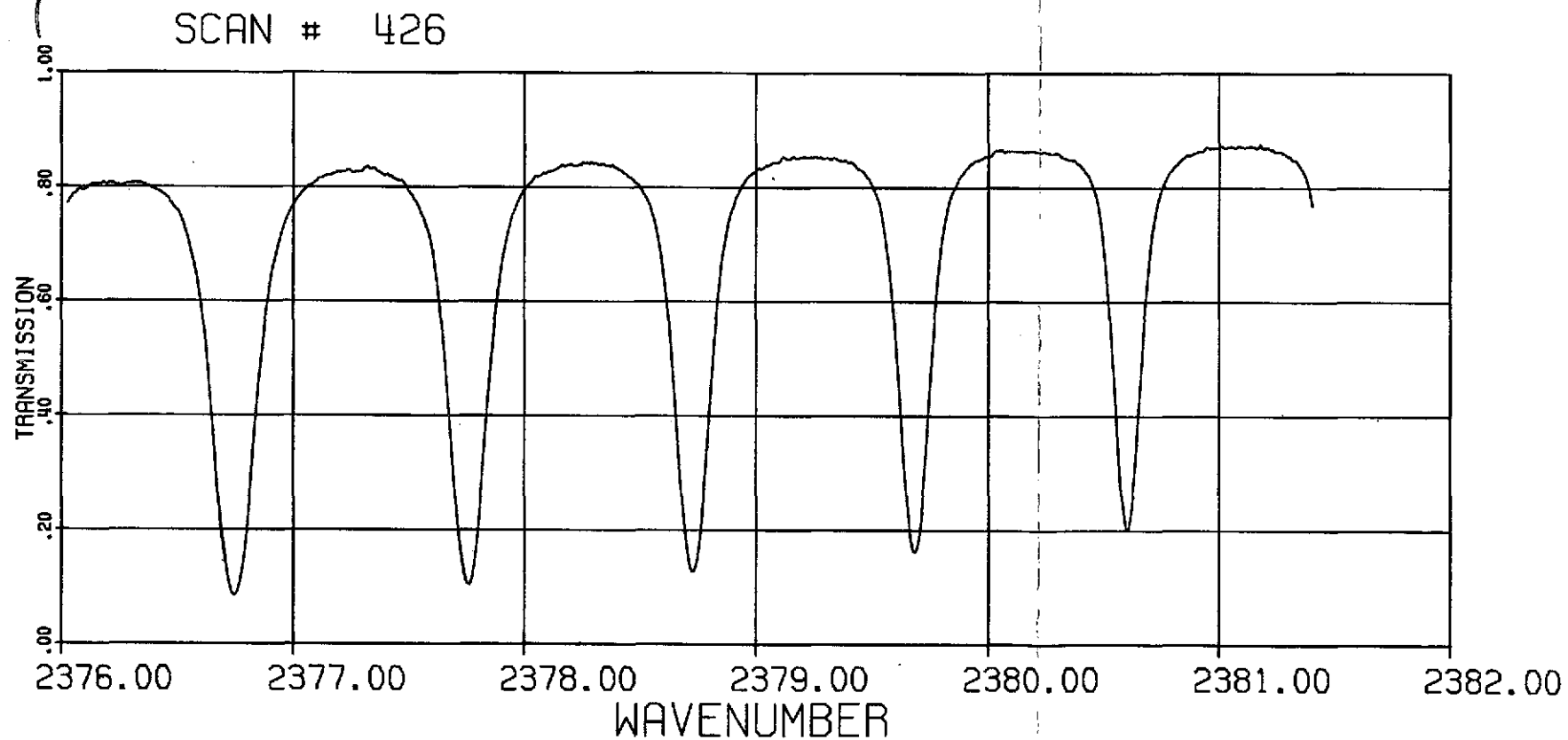


Fig. 33. Background or 100% transmission spectra used to normalize Fig. 32. Demonstrates the noise level obtained.

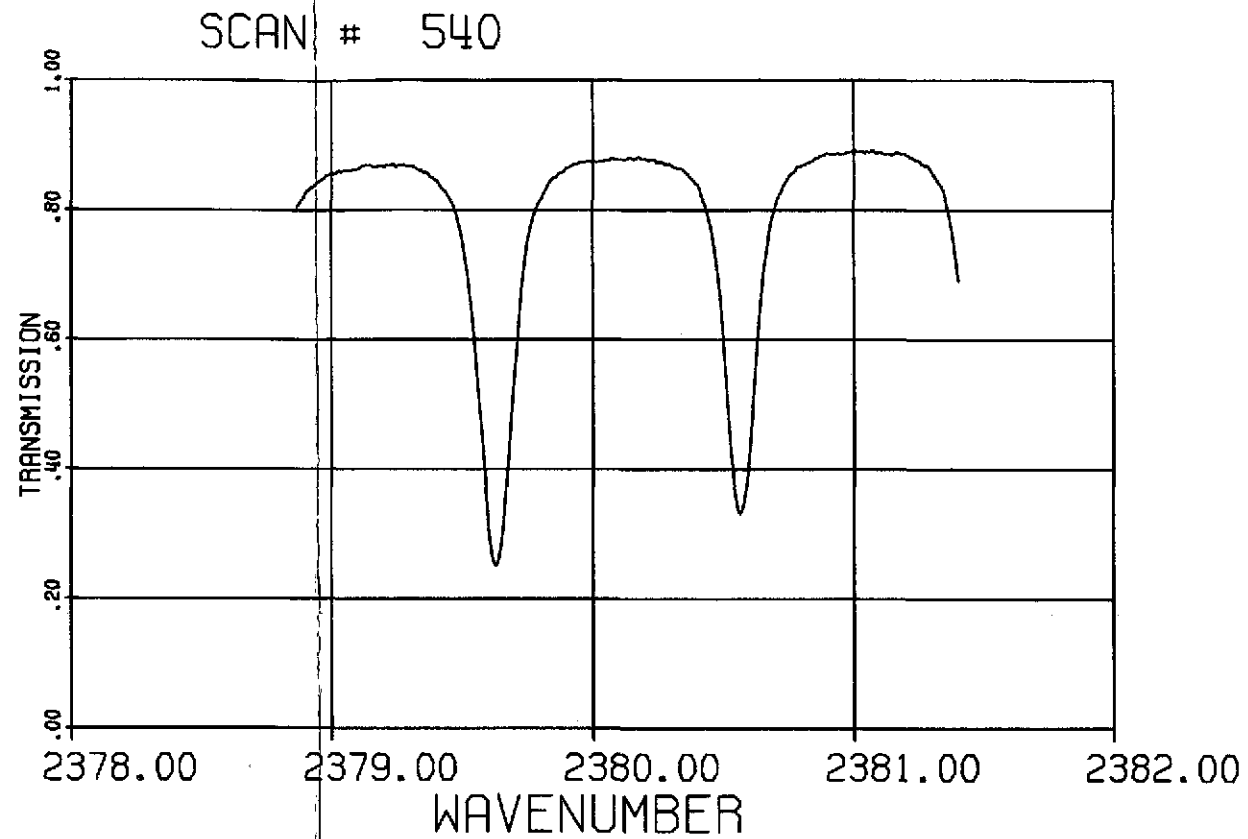
FOLDOUT FRAME



FOLDOUT FRAME 2

Fig. 34. The R branch of the  $\nu_3$  fundamental used for the self-broadening study. The isotopic and "hot" bands seen in Fig. 32 are weak in this region.  
Cell length = 8.74 cm, pressure 40.0 torr, temperatures 26.9°C.

FOLDOUT FRAME



FOLDOUT FRAME

2

Fig. 35. An example of nitrogen broadening in the same spectral region as Fig. 34. Cell length = 8.74 cm, partial pressure  $\text{CO}_2$  5.0 torr, partial pressure of  $\text{N}_2$  319 torr, temperature  $27.3^\circ\text{C}$ .

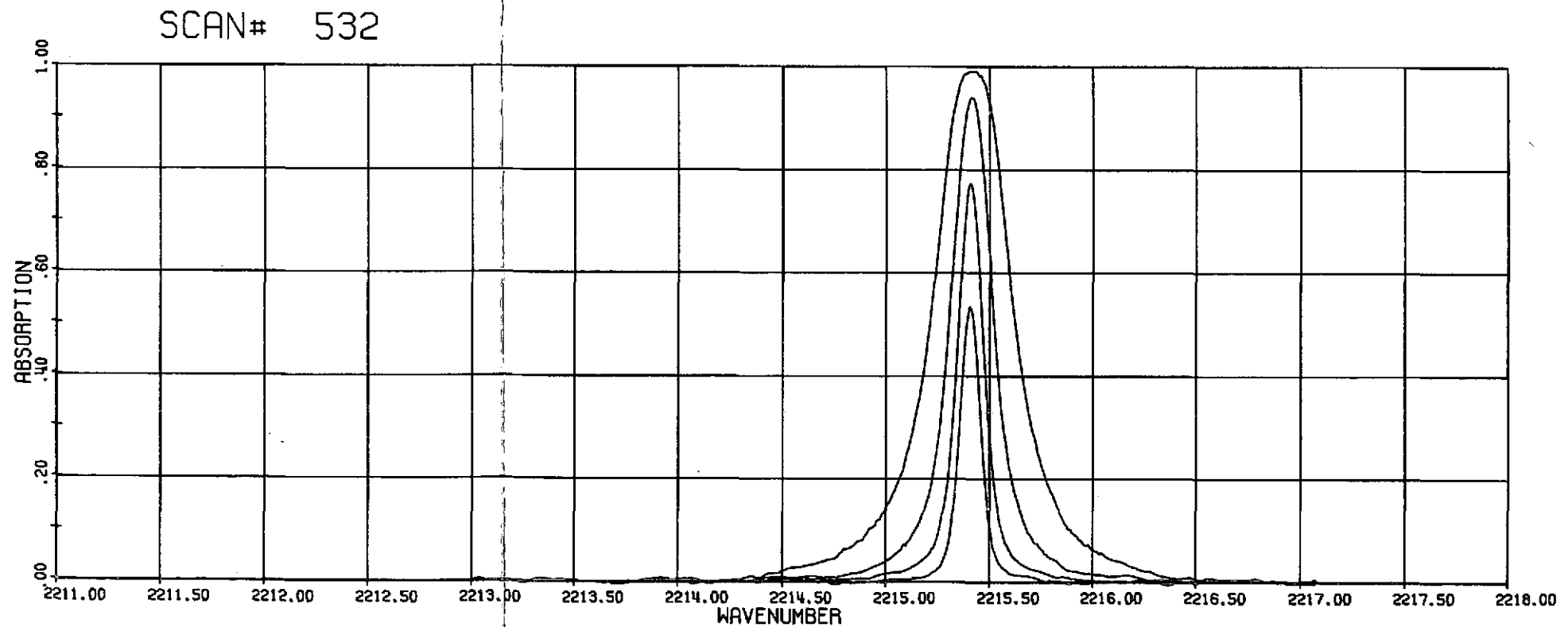


Fig. 36. Spectra of the  $\text{R}_{20}$  line of the  $4.6\mu\text{m}$  band of  $\text{CO}$ , self-broadening study. Cell length = 8.74 cm, pressure 40.0 torr, 80.0 torr, 160.0 torr, and 320 torr, temperature  $27.7^\circ\text{C}$ .

SCAN# 499

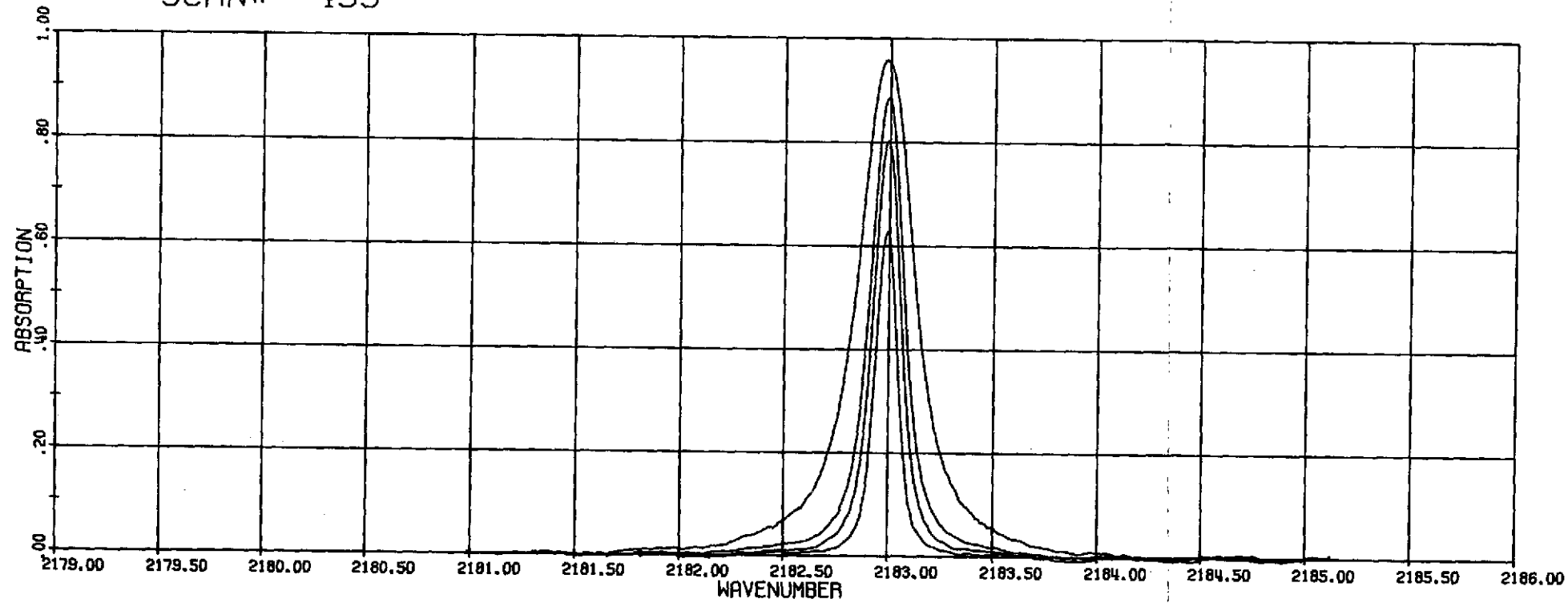


Fig. 37. Spectra of the R<sub>10</sub> line of 4.6 $\mu$ m band of CO nitrogen broadening study.  
Cell length = 8.74 cm, partial pressure of CO = 8.0 torr, partial pressure of N<sub>2</sub> = 20.3 torr, 79.6 torr, 162.2 torr, 642.7 torr.

FOLDOUT FRAME

FOLDOUT FRAME

2

SCAN# 481

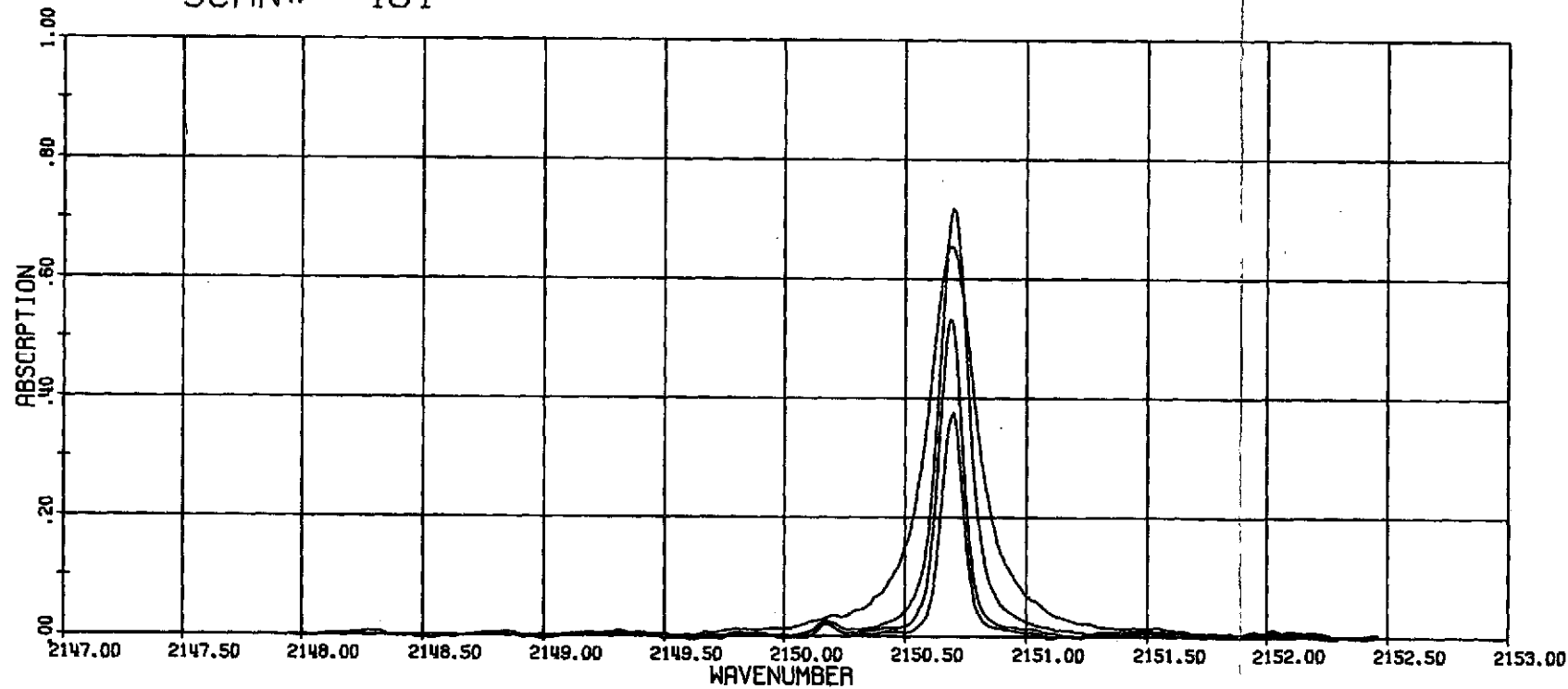


Fig. 38. Spectra of R<sub>1</sub> line of 4.6 $\mu$ m band of CO nitrogen broadening.  
Cell length = 8.74 cm, partial pressure of CO = 5.0 torr, partial pressure of nitrogen = 10.1 torr, 40.4 torr, 160.9 torr, 644.2 torr, temperature 27.1°C.

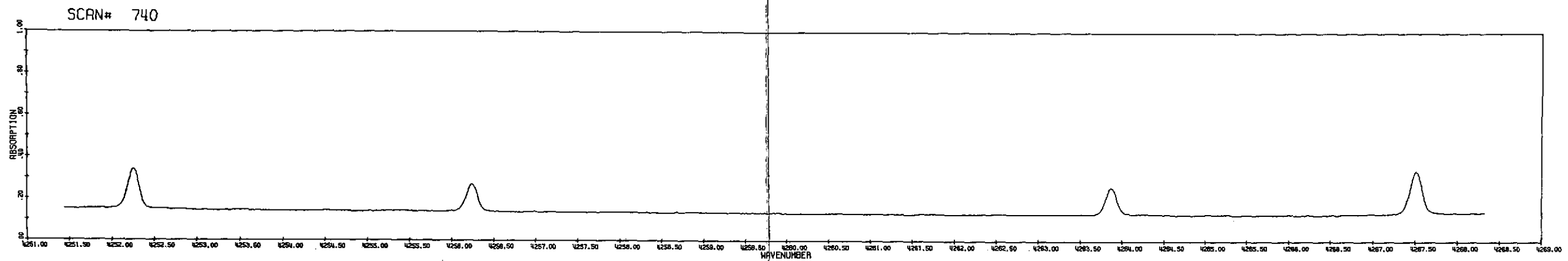


Fig. 39. Example of a partial spectrum of the  $2.3\mu\text{m}$  band of CO across the center of the band.  
Cell length = 300 cm, partial pressure of CO = 5.0 torr, partial pressure of  $\text{N}_2$  = 75.0 torr, temperature  $25.0^\circ\text{C}$ .

FOLDOUT FRAME 1

FOLDOUT FRAME 2